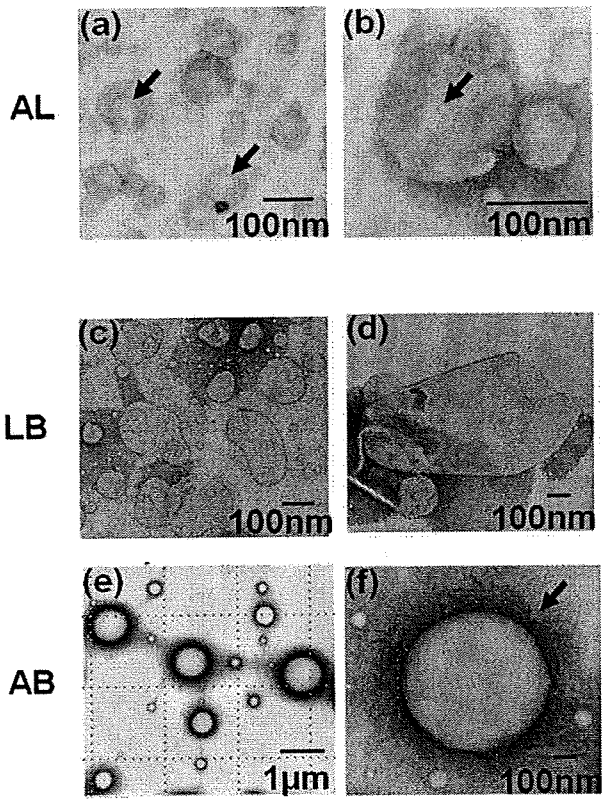

Fig. 3. Three types of ultrasound contrast agent from negative staining. AL: (a) ×50 000, (b) ×100 000. LB: (c) ×15 000, (d) ×10 000. AB: (e) ×3500, (f) ×20 000. The black arrows in (a) and (b) show where electron density was relatively low, indicating the presence of gas. The black arrow in (f) indicates albumin in filament form. (a)–(f) were stained at room temperature. (a), (b) JEOL JEM2000EX operated at 100 kV. (c)–(f) H-7600 operated at 80 kV.

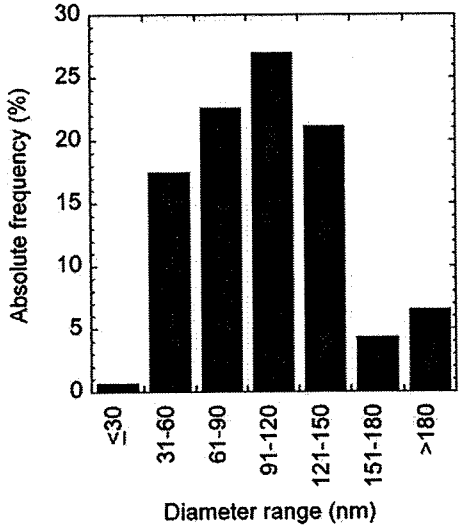

Fig. 4. Histogram of the absolute frequency distribution. The data were obtained from 10 TEM images. The maximum value was obtained within the class interval of 91–120 nm.

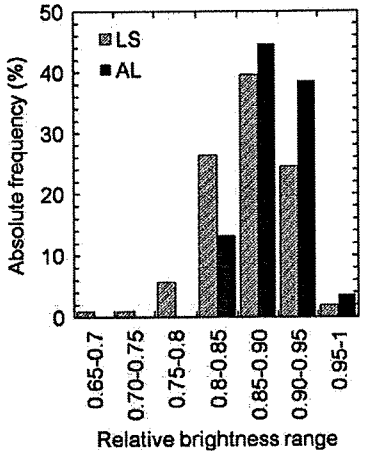

Fig. 5. Relative brightness range. AL and LS TEM micrographs were analyzed to assess the average brightness value of the inside of each kind of liposome. The inner area of each liposome image was digitally selected to measure its mean brightness value. Relative brightness values (measured mean brightness/background brightness) were obtained for 106 LSs and 83 ALs. The statistical distribution of ALs is slightly shifted to relative brightness values closer to 1 compared to the distribution of LSs, indicating that gas bubbles are actually present inside some of the ALs.

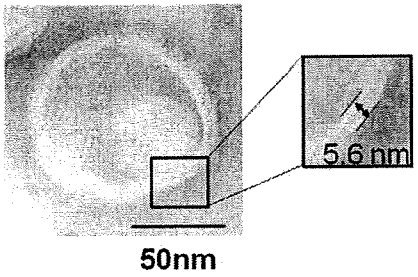

Fig. 6. Shell structure of AL. TEM micrograph of AL, negatively stained at 80°C. The distance between two lines in the magnified figure was 5.6 nm, indicating a single lipid bilayer. Original magnification, ×50 000. JEOL JEM2000EX operated at 100 kV.

AL was 24% (17 out of 70 liposomes). This value was similar to the 20% obtained and illustrated in Fig. 3a and b. Figure 7b shows that some ALs have an equal volume occupied by liquid and gas. The white arrows indicate the outside boundary, while the black arrows indicate the inside boundary. G shows the presence of gas, and L the presence of liquid. It is hard to judge whether the interface between the gas and the liquid within the AL is a gas/liquid interface or a lipid interface. Figure 7c shows an AL primarily occupied by gas. The proportion of gas relative to liquid is likely to vary depending on how the cross-section is cut. Figure 7d shows a liposome which was not sonicated, with a liquid-filled inside.

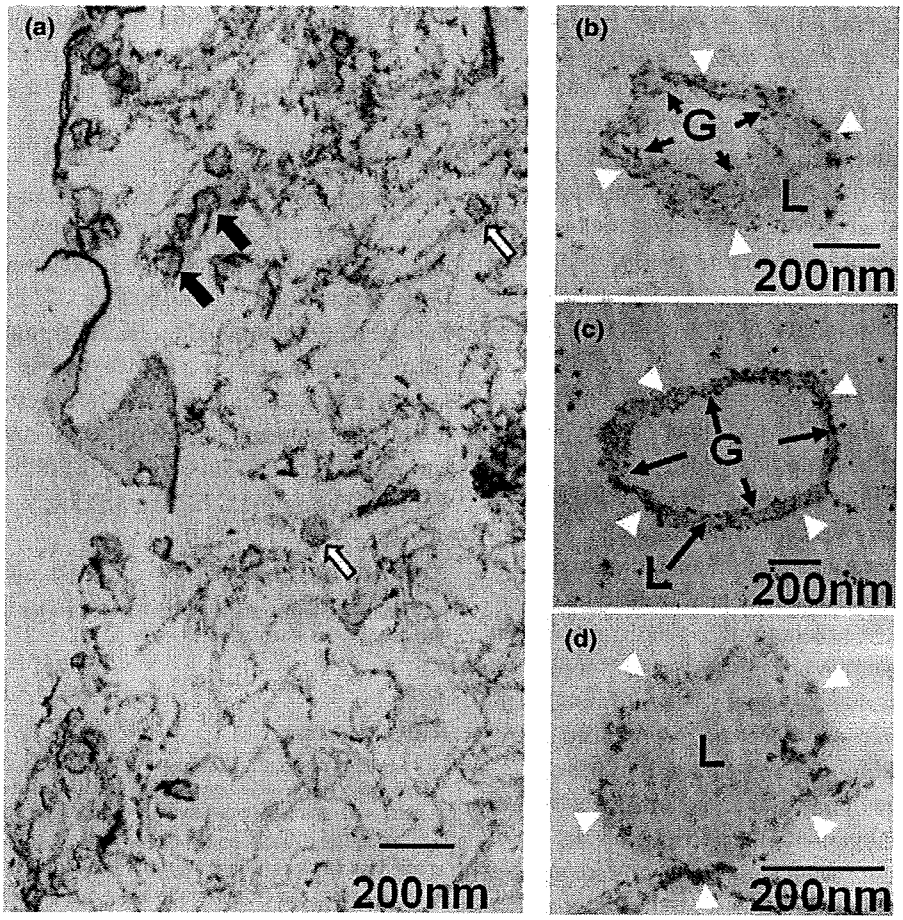

Fig. 7. Structure of AL from double staining. (a) The black arrows indicate the presence of gas in AL, while the white arrow indicates liquid. Original magnification: ×20 000. (b) AL occupied by ~50% (v/v) gas (G) and 50% (v/v) liquid (L). The white arrows indicate the outside boundary, while the black arrows indicate the inside boundary. Original magnification: ×30 000. (c) AL occupied mainly by gas (G). The liquid (L) portion was small. The white arrow indicates the outside boundary, while the black arrow indicates the inside boundary. Original magnification: ×20 000. (d) Liposome, which was not sonicated. The inside was filled with liquid (L). The white arrows indicate the outside boundary. Original magnification: ×50 000. (a)–(d) were obtained with JEOL JEM2000EX operated at 100 kV.

Discussion

The structure of an AL was investigated using TEM, and was compared with that for LB and AB. First we measured the diameter of AL by dynamic light scattering. The diameter of AL was ~200 nm (Table 1), which was about double the diameter calculated from the analysis of 10 TEM micrographs (Fig. 4). With dynamic light scattering, the size was measured immediately after AL production. TEM measurement indicated that the size of AL may have been influenced by the staining process and repeated electron beam exposure. These external factors might shift the frequency distribution to the lower value.

The zeta potential was derived from the hypothesis that ALs, LBs and ABs are hard particles [15]. ALs and LBs were found to be almost neutral, whereas AB had strong negative values (Table 1). As can be seen in TEM images (Fig. 3e and f), the electron beams were strongly scattered around the shell surface of the ABs. The key component of AB, albumin, was detected in its filament form. Ohshima [15] reported that the Smoluchowski equation cannot be applied to soft particles such as red blood cells, i.e. particles with an electric surface charge boundary in which a slip line exists. ABs are most likely to be a type of soft particle, for which this equation cannot be applied. Equations taking into account the properties of this kind of particles should be investigated.

From negative staining observations, it was assumed that AL have a single lipid bilayer as a shell structure (Fig. 6). The percentage of AL in which the presence of gas was detected was ~20%, and the proportion of volume occupied by gas and liquid varied depending on how the cross-sections were cut. Although it was hard to quantify the percentage of gas occupying the interior of AL due to the limited number of TEM images, it was clear from echogenicity that the C_3F_8 gas was actually encapsulated in ALs (Figs. 2 and 5).

Several acoustic liposome structures have been suggested [17,18]. Huang *et al.* [17] proposed that the internal volume was occupied by air and liquid compartments, and that the interface between the air and liquid compartments was a lipid monolayer. Suzuki *et al.* [18] suggested that both liquid and unilamellar lipids containing air were encapsulated by a single lipid bilayer. In the present study, we observed that gas and liquid seemed to be encapsulated together by a single lipid bilayer. However, we could not judge whether the interface between the gas and the liquid was the gas/liquid interface or the lipid interface.

The co-existence of gas and liquid in ALs provides evidence of its echogenicity and drug-carrying capabilities. Further, the tissue specificity of ALs can be improved by conjugating ligands against the target tissue with PEG on the AL surface. Recently, a high-frequency ultrasound system with ALs has been developed and applied so far to the imaging of anterior segment of the eye [19], skin [20] and tumor vasculature [21]. Studies have shown that the permeability of the tumor vasculature is enhanced, and the phenomenon is recognized as the EPR effect [11].

Most anticancer drugs have diameters of 10–120 nm: Genexol-PM (20–50 nm in diameter), Doxil (80–90 nm in diameter), Abraxane (120 nm in diameter) [12]. Sonoporation delivery efficiency, *in vivo* behavior and tissue-specificity of ALs would possibly be enhanced if the diameter was controlled within the range of 10–120 nm, the surface was positively or negatively charged, and ligands against the tumor were conjugated to PEG on the surface [22–24].

Concluding remarks

In summary, the findings of the present study indicate that AL have a shell consisting of a single lipid bilayer and can encapsulate both drugs and gas. The PEG distributed over the surface can be conjugated with tissue-specific ligands. Developing functional AL will assure the effectiveness of sonoporation.

Funding

This work was supported by a Grant-in-Aid for Scientific Research (B) [20300173 to T.K., 19390507 to S.M.]; a Grant-in-Aid for Scientific Research on Priority Area, MEXT [20015005 to T.K.]; a Grant for Research on Advanced Medical Technology, the Ministry of Health, Labor and Welfare of Japan [H19-nano-010 to T.K.]; a Grant for Research on Development of Systems and Technology for Advanced Measurement and Analysis, JST [T.K.]; and a Grant-in-Aid for JSPS Fellows [21-7271 to S.H.].

Acknowledgements

The authors would like to thank Yukiko Watanabe, Rui Chen and Li Li, for their technical assistance.

References

1 Kodama T, Tomita Y, Koshiyama K, and Blomley M J (2006) Transfection effect of microbubbles on cells in superposed ultrasound waves and behavior of cavitation bubble. *Ultrasound Med. Biol.* **32**: 905–914.

2 Lindner J R (2004) Microbubbles in medical imaging: current applications and future directions. *Nat. Rev. Drug Discov.* **3**: 527–532.

3 Shohet R V, Chen S, Zhou Y T, Wang Z, Meidell R S, Unger R H, and Grayburn P A (2000) Echocardiographic destruction of albumin microbubbles directs gene delivery to the myocardium. *Circulation* **101**: 2554–2556.

4 Christiansen J P, French B A, Klibanov A L, Kaul S, and Lindner J R (2003) Targeted tissue transfection with ultrasound destruction of plasmid-bearing cationic microbubbles. *Ultrasound Med. Biol.* **29**: 1759–1767.

5 Suzuki R, Takizawa T, Negishi Y, Utoguchi N, Sawamura K, Tanaka K, Namai E, Oda Y, Matsumura Y, and Maruyama K (2008) Tumor specific ultrasound enhanced gene transfer *in vivo* with novel liposomal bubbles. *J. Control. Release* **125**: 137–144.

6 Suzuki R, Oda Y, Utoguchi N, Namai E, Taira Y, Okada N, Kadowaki N, Kodama T, Tachibana K, and Maruyama K (2009) A novel strategy utilizing ultrasound for antigen delivery in dendritic cell-based cancer immunotherapy. *J. Control. Release* **133**: 198–205.

7 Church C C (1995) The effrcts of an elastic solid-surface layer on the radial pulsations of gas-bubbles. *J. Acoust. Soc. Am.* **97**: 1510–1521.

8 Kodama T, Tomita Y, Watanabe Y, Koshiyama K, Yano T, and Fujikawa S (2009) Cavitation bubbles mediated molecular delivery during sonoporation. *J. Biomech. Sci. Eng.* **4**: 124–140.

9 Suzuki R, Takizawa T, Negishi Y, Hagisawa K, Tanaka K, Sawamura K, Utoguchi N, Nishioka T, and Maruyama K (2007) Gene delivery by combination of novel liposomal bubbles with perfluoropropane and ultrasound. *J. Control. Release* **117**: 130–136.

10 Klibanov A L, Maruyama K, Torchilin V P, and Huang L (1990) Amphipathic polyethyleneglycols effectively prolong the circulation time of liposomes. *FEBS Lett.* **268**: 235–237.

11 Matsumura Y and Maeda H (1986) A new concept for macromolecular therapeutics in cancer chemotherapy: mechanism of tumoritropic

accumulation of proteins and the antitumor agent smancs. *Cancer Res.* **46**: 6387–6392.

12 Davis M E, Chen Z G, and Shin D M (2008) Nanoparticle therapeutics: an emerging treatment modality for cancer. *Nat. Rev. Drug Discov.* **7**: 771–782.

13 Aoi A, Watanabe Y, Mori S, Takahashi M, Vassaux G, and Kodama T (2008) Herpes simplex virus thymidine kinase-mediated suicide gene therapy using nano/microbubbles and ultrasound. *Ultrasound Med. Biol.* **34**: 425–434.

14 Watanabe Y, Aoi A, Horie S, Tomita N, Mori S, Morikawa H, Matsumura Y, Vassaux G, and Kodama T (2008) Low-intensity ultrasound and microbubbles enhance the antitumor effect of cisplatin. *Cancer Sci.* **99**: 2525–2531.

15 Ohshima H (1994) Electrophoretic mobility of soft particles. *J. Colloid Interface Sci.* **163**: 474–483.

16 Yanai H (2007) *Statcel—The Useful Add-in Forms on Excel.* (OMS, Tokyo).

17 Huang S L, and Macdonald R C (2004) Acoustically active liposomes for drug encapsulation and ultrasound-triggered release. *Biochim. Biophys. Acta* **1665**: 134–141.

18 Suzuki R, Takizawa T, Negishi Y, Utoguchi N, and Maruyama K (2008) Effective gene delivery with novel liposomal bubbles and ultrasonic destruction technology. *Int. J. Pharm.* **354**: 49–55.

19 Pavlin C J, and Foster F S (1998) Ultrasound biomicroscopy. High-frequency ultrasound imaging of the eye at microscopic resolution. *Radiol. Clin. North Am.* **36**: 1047–1058.

20 Vogt M, and Ermert H (2008) Limited-angle spatial compound imaging of skin with high-frequency ultrasound (20 MHz). *IEEE Trans. Ultrason. Ferroelectr. Freq Control* **55**: 1975–1983.

21 Lyshchik A, Fleischer A C, Huamani J, Hallahan D E, Brissova M, and Gore J C (2007) Molecular imaging of vascular endothelial growth factor receptor 2 expression using targeted contrast-enhanced high-frequency ultrasonography. *J. Ultrasound Med.* **26**, 1575–1586.

22 Schneider M (2008) Molecular imaging and ultrasound-assisted drug delivery. *J. Endourol.* **22**: 795–802.

23 Kaufmann B A, and Lindner J R (2007) Molecular imaging with targeted contrast ultrasound. *Curr. Opin. Biotechnol.* **18**: 11–16.

24 Palmowski M, Huppert J, Hauff P, Reinhardt M, Schreiner K, Socher M A, Hallscheidt P, Kauffmann G W, Semmler W, and Kiessling F (2008) Vessel fractions in tumor xenografts depicted by flow- or contrast-sensitive three-dimensional high-frequency Doppler ultrasound respond differently to antiangiogenic treatment. *Cancer Res.* **68**: 7042–7049.

molecular pharmaceutics

articles

Enhanced Laminin-Derived Peptide AG73-Mediated Liposomal Gene Transfer by Bubble Liposomes and Ultrasound

Yoichi Negishi,*[,†,‡] Daiki Omata,[†,‡] Hiroshi Iijima,[†] Yasuko Takabayashi,[†] Kentaro Suzuki,[†] Yoko Endo,[†] Ryo Suzuki,[§] Kazuo Maruyama,[§] Motoyoshi Nomizu,[∥] and Yukihiko Aramaki[†]

Drug and Gene Delivery Systems, School of Pharmacy, Tokyo University of Pharmacy and Life Sciences, Hachioji, Tokyo 192-0392, Japan, Biopharmaceutics, School of Pharmaceutical Sciences, Teikyo University, Sagamihara, Kanagawa 229-0915, Japan, and Clinical Biochemistry, School of Pharmacy, Tokyo University of Pharmacy and Life Sciences, Hachioji, Tokyo 192-0392, Japan

Received August 28, 2009; Revised Manuscript Received November 13, 2009; Accepted December 18, 2009

Abstract: A promising strategy as a cancer therapeutic is tumor-targeted gene delivery. The AG73 peptide derived from the laminin α1 chain is a ligand for syndecans, and syndecan-2 is highly expressed in some cancer cells. In this study, AG73-PEG liposomes were developed for selective gene delivery to syndecan-2 overexpressing cancer cells. AG73-PEG liposomes were used in combination with Bubble liposomes and ultrasound exposure to enhance transfection efficiency by promoting the escape of the liposomes from the endosome to the cytosol. AG73-PEG liposomes showed selective gene delivery to syndecan-2 overexpressing cancer cells. Furthermore, AG73-mediated liposomal gene transfection efficiency was enhanced by 60-fold when Bubble liposomes and ultrasound exposure were used, despite the absence of an increase in the uptake of AG73-PEG liposomes into the cells. Confocal microscope analysis revealed that the Bubble liposomes and ultrasound promoted intracellular trafficking of the AG73-PEG liposomes during gene transfection. Thus, the combination of AG73-PEG liposomes with Bubble liposomes and ultrasound exposure may be a promising method to achieve selective and efficient gene delivery for cancer therapy.

Keywords: AG73 peptide; Bubble liposomes; gene delivery; syndecan-2; ultrasound

Introduction

The success of human gene therapy depends upon the development of delivery vehicles or vectors that can selectively deliver therapeutic genes to target cells safely and with high efficiency. There are two main approaches in gene delivery, namely, viral gene delivery and nonviral gene delivery. Although viral vectors have high transfection efficiencies over a wide range of cell targets, they have major limitations, including virally induced inflammatory responses and oncogenic effects.[1,2] Nonviral vectors, which are generally delivered as a complex with chemical and/or biochemical

* Corresponding author. Mailing address: Tokyo University of Pharmacy and Life Sciences, School of Pharmacy, Drug and Gene Delivery Systems, 1432-1 Horinouchi, Hachioji, Tokyo 192-0392, Japan. Tel and fax: +81-42-676-3183. E-mail: negishi@ps.toyaku.ac.jp.

† Drug and Gene Delivery Systems, School of Pharmacy, Tokyo University of Pharmacy and Life Sciences.

‡ The first two authors contributed equally to this work.

§ Teikyo University.

∥ Clinical Biochemistry, School of Pharmacy, Tokyo University of Pharmacy and Life Sciences.

10.1021/mp900214s © 2010 American Chemical Society
Published on Web 12/18/2009

(1) Dewey, R. A.; Morrissey, G.; Cowsill, C. M.; Stone, D.; Bolognani, F.; Dodd, N. J.; Southgate, T. D.; Klatzmann, D.; Lassmann, H.; Castro, M. G.; Löwenstein, P. R. Chronic brain inflammation and persistent herpes simplex virus 1 thymidine kinase expression in survivors of syngeneic glioma treated by adenovirus-mediated gene therapy: implications for clinical trials. *Nat. Med.* **1999**, *5*, 1256–1263.

vectors such as cationic lipids or polymers, continue to be an attractive alternative to viral vectors due to their safety, versatility, and ease of preparation and scale-up. Nonviral vectors, however, generally suffer from relatively low transfection efficiencies.[3,4]

A promising strategy for enhancing cancer gene therapy is tumor-targeted gene delivery. Some targeting moieties have been used in studies for cancer gene therapy, such as transferrin, folate, anisamide, RGD-peptides, and antibodies.[5−10]

The present study focused on AG73, which is 12 amino acid synthetic peptide derived from the globular domain of the laminin α1 chain. AG73 peptide is a ligand for syndecans, one of the major heparan sulfate-containing transmembrane proteoglycans.[11−13] Syndecan-2 is highly expressed in various cancer cell lines and plays a role in angiogenesis.[14−18] Therefore, AG73-labeled polyethyleneglycol-modified liposomes (AG73-PEG liposomes) were developed, which are capable of encapsulating a gene condensed by poly-L-lysine. However, PEG modification of liposomes can enhance the stability of pDNA in serum and also suppress the association of liposomes with cells or cause endosomal escape of liposomes, leading to a decrease in transfection efficiency.[19−23]

A novel approach to the administration of a drug or gene is the use of ultrasound (US)-enhanced delivery. US-enhanced delivery exploits the cavitation bubbles produced by the pressure oscillations of US. Furthermore, US waves above a certain threshold can cause oscillating bubbles to undergo a violent collapse known as inertial cavitation. Inertial cavitation is believed to enhance the permeability of a tissue or a cell membrane transiently.[24−28] Microbubbles, which are contrast agents for medical US imaging, improve

(2) Sun, J. Y.; Anand-Jawa, V.; Chatterjee, S.; Wong, K. K. Immune responses to adeno-associated virus and its recombinant vectors. *Gene Ther.* **2003**, *10*, 964–976.
(3) Audouy, S. A.; de Leij, L. F.; Hoekstra, D.; Molema, G. In vivo characteristics of cationic liposomes as delivery vectors for gene therapy. *Pharm. Res.* **2002**, *19*, 1599–1605.
(4) Hirko, A.; Tang, F.; Hughes, J. A. Cationic lipid vectors for plasmid DNA delivery. *Curr. Med. Chem.* **2003**, *10*, 1185–1193.
(5) Leamon, C. P.; Weigl, D.; Hendren, R. W. Folate copolymer-mediated transfection of cultured cells. *Bioconjugate Chem.* **1999**, *10*, 947–957.
(6) Merdan, T.; Callahan, J.; Petersen, H.; Kunath, K.; Bakowsky, U.; Kopecková, P.; Kissel, T.; Kopecek, J. Pegylated polyethylenimine-Fab' antibody fragment conjugates for targeted gene delivery to human ovarian carcinoma cells. *Bioconjugate Chem.* **2003**, *14*, 989–996.
(7) Li, S. D.; Huang, L. Targeted delivery of antisense oligodeoxynucleotide and small interference RNA into lung cancer cells. *Mol. Pharmaceutics* **2006**, *3*, 579–588.
(8) Suk, J. S.; Suh, J.; Choy, K.; Lai, S. K.; Fu, J.; Hanes, J. Gene delivery to differentiated neurotypic cells with RGD and HIV Tat peptide functionalized polymeric nanoparticles. *Biomaterials* **2006**, *27*, 5143–5150.
(9) Li, S. D.; Chen, Y. C.; Hackett, M. J.; Huang, L. Tumor-targeted delivery of siRNA by self-assembled nanoparticles. *Mol. Ther.* **2008**, *16*, 163–169.
(10) Pirollo, K. F.; Rait, A.; Zhou, Q.; Zhang, X. Q.; Zhou, J.; Kim, C. S.; Benedict, W. F.; Chang, E. H. Tumor-targeting nanocomplex delivery of novel tumor suppressor RB94 chemosensitizes bladder carcinoma cells in vitro and in vivo. *Clin. Cancer Res.* **2008**, *14*, 2190–2198.
(11) Carey, D. J. Syndecans: multifunctional cell-surface co-receptors. *Biochem. J.* **1997**, *327*, 1–16.
(12) Hoffman, M. P.; Nomizu, M.; Roque, E.; Lee, S.; Jung, D. W.; Yamada, Y.; Kleinman, H. K. Laminin-1 and laminin-2 G-domain synthetic peptides bind syndecan-1 and are involved in acinar formation of a human submandibular gland cell line. *J. Biol. Chem.* **1998**, *273*, 28633–28641.
(13) Suzuki, N.; Ichikawa, N.; Kasai, S.; Yamada, M.; Nishi, N.; Morioka, H.; Yamashita, H.; Kitagawa, Y.; Utani, A.; Hoffman, M. P.; Nomizu, M. Syndecan binding sites in the laminin alpha1 chain G domain. *Biochemistry* **2003**, *42*, 12625–12633.
(14) Han, I.; Park, H.; Oh, E. S. New insights into syndecan-2 expression and tumourigenic activity in colon carcinoma cells. *J. Mol. Histol.* **2004**, *35*, 319–326.
(15) Tkachenko, E.; Rhodes, J. M.; Simons, M. Syndecans: new kids on the signaling block. *Circ. Res.* **2005**, *96*, 488–500.
(16) Essner, J. J.; Chen, E.; Ekker, S. C. Syndecan-2. Int. J. Biochem. *Cell Biol.* **2006**, *38*, 152–156.
(17) Fears, C. Y.; Woods, A. The role of syndecans in disease and wound healing. *Matrix Biol.* **2006**, *25*, 443–456.
(18) Noguer, O.; Villena, J.; Lorita, J.; Vilaró, S.; Reina, M. Syndecan-2 downregulation impairs angiogenesis in human microvascular endothelial cells. *Exp. Cell Res.* **2009**, *315*, 795–808.
(19) Zalipsky, S.; Qazen, M.; Walker, J. A.; Mullah, N.; Quinn, Y. P.; Huang, S. K. New detachable poly(ethylene glycol) conjugates: cysteine-cleavable lipopolymers regenerating natural phospholipid, diacyl phosphatidylethanolamine. *Bioconjugate Chem.* **1999**, *10*, 703–707.
(20) Guo, X.; Szoka, F. C. Steric stabilization of fusogenic liposomes by a low-pH sensitive PEG--diortho ester--lipid conjugate. *Bioconjugate Chem.* **2001**, *12*, 291–300.
(21) Shin, J.; Shum, P.; Thompson, D. H. Acid-triggered release via dePEGylation of DOPE liposomes containing acid-labile vinyl ether PEG-lipids. *J. Controlled Release* **2003**, *91*, 187–200.
(22) Walker, G. F.; Fella, C.; Pelisek, J.; Fahrmeir, J.; Boeckle, S.; Ogris, M.; Wagner, E. Toward synthetic viruses: endosomal pH-triggered deshielding of targeted polyplexes greatly enhances gene transfer in vitro and in vivo. *Mol. Ther.* **2005**, *11*, 418–425.
(23) Hatakeyama, H.; Akita, H.; Kogure, K.; Oishi, M.; Nagasaki, Y.; Kihira, Y.; Ueno, M.; Kobayashi, H.; Kikuchi, H.; Harashima, H. Development of a novel systemic gene delivery system for cancer therapy with a tumor-specific cleavable PEG-lipid. *Gene Ther.* **2007**, *14*, 68–77.
(24) Holmes, R. P.; Yeaman, L. D.; Taylor, R. G.; McCullough, D. L. Altered neutrophil permeability following shock wave exposure in vitro. *J. Urol.* **1992**, *147*, 733–737.
(25) Greenleaf, W. J.; Bolander, M. E.; Sarkar, G.; Goldring, M. B.; Greenleaf, J. F. Artificial cavitation nuclei significantly enhance acoustically induced cell transfection. *Ultrasound Med. Biol.* **1998**, *24*, 587–595.
(26) Delius, M.; Adams, G. Shock wave permeabilization with ribosome inactivating proteins: a new approach to tumor therapy. *Cancer Res.* **1999**, *59*, 5227–5232.
(27) Schratzberger, P.; Krainin, J. G.; Schratzberger, G.; Silver, M.; Ma, H.; Kearney, M.; Zuk, R. F.; Brisken, A. F.; Losordo, D. W.; Isner, J. M. Transcutaneous ultrasound augments naked DNA transfection of skeletal muscle. *Mol. Ther.* **2002**, *6*, 576–583.
(28) Duvshani-Eshet, M.; Machluf, M. Therapeutic ultrasound optimization for gene delivery: a key factor achieving nuclear DNA localization. *J. Controlled Release* **2005**, *108*, 513–528.

permeability after US-induced cavitation.[29−34] However, microbubbles have problems associated with their size, stability, and targeting function. Therefore, the present study developed echo-contrast gas entrapping liposomes, also known as Bubble liposomes (BLs). We found that BLs and US exposure could enhance the permeability of a tissue or the cell membrane transiently.[35−38] We hypothesized that BLs and US may affect not only the cell membrane but also intracellular vesicles and could enhance the escape of pDNA from endosomes to the cytoplasm.

This study assessed the selectivity of AG73-PEG liposomes for syndecan-2 overexpressing cells and examined whether AG73-mediated liposomal gene transfection could be enhanced by BLs and US exposure to achieve highly efficient transfection.

Experimental Section

Materials. The plasmid pCMV-Luc is an expression vector encoding the firefly luciferase gene under the control of a cytomegalovirus promoter. Chloroquine was purchased from Sigma (St. Louis, MO). Cy3-labeled pDNA was purchased from Mirus Bio LLC, Madison, WI. Alexa Fluor 488-conjugated transferrin was purchased from Molecular Probes, Inc. (Eugene, OR).

Cell Lines and Cultures. A 293T human embryonic kidney carcinoma cell line, stably overexpressing syndecan-2 (293T-Syn2 cell), was cultured in Dulbecco's modified Eagle's medium (DMEM; Kohjin Bio Co. Ltd., Tokyo, Japan), supplemented with 10% fetal bovine serum (FBS; Equitech Bio Inc., Kerrville, TX), penicillin (100 U/mL), streptomycin (100 μg/mL), and puromycin (0.4 μg/mL), at 37 °C in a humidified 5% CO_2 atmosphere.

Preparation of AG73-PEG Liposomes. The Cys-AG73 peptide (CGG-RKRLQVQLSIRT) and scrambled Cys-AG73T control peptide (CGG-LQQRRSVLRTKI) were synthesized manually using the 9-fluorenylmethoxycarbonyl (Fmoc)-based solid-phase strategy, prepared in the COOH-terminal amide form and purified by reverse-phase high-performance liquid chromatography. AG73-labeled PEG liposomes were prepared by the hydration method. pDNA diluted in 10 mM HEPES buffer (pH 7.4) (0.1 mg/mL) was condensed using poly-L-lysine (PLL) (0.1 mg/mL) (SIGMA-Aldrich Co., St. Louis, MO). The complex of pDNA and PLL was added to a lipid film composed of 1,2-dioleoyl-*sn*-glycero-3-phospho-*rac*-1-glycerol (DOPG) (AVANTI Polar Lipids Inc., Alabaster, AL), 1,2-dioleoyl-*sn*-glycero-3-phosphoethanolamine (DOPE) (AVANTI Polar Lipids Inc., Alabaster, AL), and 1,2-distearoyl-*sn*-glycero-3-phosphatidylethanolamine-polyethyleneglycol-maleimide (DSPE-PEG_{2000}-Mal) in a molar ratio of 2:9:0.57, followed by incubation for 10 min at room temperature to hydrate the lipids. The solution was sonicated for 5 min in a bath-type sonicator (42 kHz, 100 W) (BRANSONIC 2510J-DTH, Bransoni Ultrasonic Co., Danbury, CT). For coupling, AG73 peptide, at a molar ratio of 5-fold DSPE-PEG_{2000}-Mal, was added to the PEG liposomes, and the mixture was incubated for 6 h at room temperature to conjugate cysteine of Cys-AG73 peptide with the maleimide of the PEG liposomes using a thioether bond. The resulting AG73-peptide-conjugated PEG liposomes (AG73-PEG liposomes) were dialyzed to remove any excess peptide. AG73-PEG liposomes were modified with 5 mol % PEG and 3 mol % peptides. The peptide conjugates were confirmed by protein assay (Thermo Scientific Inc., MA).

Preparation of Bubble Liposomes. PEG liposomes composed of 1,2-dipalmitoyl-*sn*-glycero-3-phosphocholine (DPPC) (NOF Corporation, Tokyo, Japan) and 1,2-distearoyl-*sn*-glycero-3-phosphatidylethanolamine-polyethyleneglycol (DSPE-PEG_{2000}-OMe) (NOF corporation, Tokyo, Japan) in a molar ratio of 94:6 were prepared by a reverse-phase evaporation method. In brief, all reagents were dissolved in 1:1 (v/v) chloroform/diisopropyl ether. Phosphate buffered saline was added to the lipid solution, and the mixture was sonicated and then evaporated at 47 °C. The organic solvent was completely removed, and the size of the liposomes was adjusted to less than 200 nm using extruding equipment and

(29) Taniyama, Y.; Tachibana, K.; Hiraoka, K.; Aoki, M.; Yamamoto, S.; Matsumoto, K.; Nakamura, T.; Ogihara, T.; Kaneda, Y.; Morishita, R. Development of safe and efficient novel nonviral gene transfer using ultrasound: enhancement of transfection efficiency of naked plasmid DNA in skeletal muscle. *Gene Ther.* **2002**, *9*, 372–380.

(30) Taniyama, Y.; Tachibana, K.; Hiraoka, K.; Namba, T.; Yamasaki, K.; Hashiya, N.; Aoki, M.; Ogihara, T.; Yasufumi, K.; Morishita, R. Local delivery of plasmid DNA into rat carotid artery using ultrasound. *Circulation* **2002**, *105*, 1233–1239.

(31) Li, T.; Tachibana, K.; Kuroki, M.; Kuroki, M. Gene transfer with echo-enhanced contrast agents: comparison between Albunex, Optison, and Levovist in mice—initial results. *Radiology* **2003**, *229*, 423–428.

(32) Unger, E. C.; Porter, T.; Culp, W.; Labell, R.; Matsunaga, T.; Zutshi, R. Therapeutic applications of lipid-coated microbubbles. *Adv. Drug Delivery Rev.* **2004**, *56*, 1291–1314.

(33) Kinoshita, M.; Hynynen, K. A novel method for the intracellular delivery of siRNA using microbubble-enhanced focused ultrasound. *Biochem. Biophys. Res. Commun.* **2005**, *335*, 393–399.

(34) Tsunoda, S.; Mazda, O.; Oda, Y.; Iida, Y.; Akabame, S.; Kishida, T.; Shin-Ya, M.; Asada, H.; Gojo, S.; Imanishi, J.; Matsubara, H.; Yoshikawa, T. Sonoporation using microbubble BR14 promotes pDNA/siRNA transduction to murine heart. *Biochem. Biophys. Res. Commun.* **2005**, *336*, 118–127.

(35) Suzuki, R.; Takizawa, T.; Negishi, Y.; Hagisawa, K.; Tanaka, K.; Sawamura, K.; Utoguchi, N.; Nishioka, T.; Maruyama, K. Gene delivery by combination of novel liposomal bubbles with perfluoropropane and ultrasound. *J. Controlled Release* **2007**, *117*, 130–136.

(36) Negishi, Y.; Endo, Y.; Fukuyama, T.; Suzuki, R.; Takizawa, T.; Omata, D.; Maruyama, K.; Aramaki, Y. Delivery of siRNA into the cytoplasm by liposomal bubbles and ultrasound. *J. Controlled Release* **2008**, *132*, 124–130.

(37) Suzuki, R.; Takizawa, T.; Negishi, Y.; Utoguchi, N.; Maruyama, K. Effective gene delivery with novel liposomal bubbles and ultrasonic destruction technology. *Int. J. Pharm.* **2008**, *354*, 49–55.

(38) Suzuki, R.; Takizawa, T.; Negishi, Y.; Utoguchi, N.; Sawamura, K.; Tanaka, K.; Namai, E.; Oda, Y.; Matsumura, Y.; Maruyama, K. Tumor specific ultrasound enhanced gene transfer in vivo with novel liposomal bubbles. *J. Controlled Release* **2008**, *125*, 137–144.

a sizing filter (pore size: 200 nm) (Nuclepore Track-Etch Membrane, Whatman plc, U.K.). The lipid concentration was measured using a Phospholipid C test Wako (Wako Pure Chemical Industries, Ltd., Osaka, Japan). BLs were prepared from liposomes and perfluoropropane gas (Takachio Chemical Ind. Co. Ltd., Tokyo, Japan). First, 2 mL sterilized vials containing 0.8 mL of liposome suspension (lipid concentration: 1 mg/mL) were filled with perfluoropropane gas, capped, and then pressurized with a further 3 mL of perfluoropropane gas. The vial was placed in a bath-type sonicator (42 kHz, 100 W) (BRANSONIC 2510j-DTH, Branson Ultrasonics Co., Danbury, CT) for 5 min to form BLs.

Transfection of pDNA into Cells Using AG73-PEG Liposomes. The two days before the experiments, 293T-Syn2 cells (1×10^5) were seeded in a 48-well plate. The cells were treated with AG73-PEG liposomes (encapsulated pDNA: 3 μg/mL) in serum-free medium for 4 h at 37 °C. After replacement with fresh medium, the cells were cultured for 20 h and then luciferase activity was measured.

Transfection of pDNA into Cells by Combination of AG73-PEG Liposomes with BLs and US Exposure. The two days before the experiments, 293T-Syn2 cells (1×10^5) were seeded in a 48-well plate. The cells were treated with AG73-PEG liposomes (encapsulated pDNA: 3 μg/mL) in serum-free medium for 4 h at 37 °C. After incubation, the cells were washed twice to remove any excess AG73-PEG liposomes that were not associated with the cells and BLs (120 μg/mL) were added. Then, US exposure was applied through a 6 mm diameter probe placed in the well (frequency, 2 MHz; duty, 50%; burst rate, 2 Hz; intensity, 1.0 W/cm^2; time, 10 s). A Sonopore 3000 (NEPA GENE, CO., Ltd., Chiba, Japan) was used to generate the US exposure. The cells were cultured for 20 h, and then luciferase activity was determined and cell viability was measured using an MTT assay.

Measurement of Luciferase Expression. Cell lysate was prepared with a lysis buffer (0.1 M Tris-HCl (pH 7.8), 0.1% Triton X-100, and 2 mM EDTA). Luciferase activity was measured using a luciferase assay system (Promega, Madison, WI) and a luminometer (LB96 V, Belthold Japan Co. Ltd., Tokyo, Japan). The activity is indicated as relative light units (RLU) per mg protein.

Flow Cytometry Analysis. The two days before the experiments, 293T-Syn2 cells (2×10^5) were seeded in a 24-well plate. 0.2 mol % Rhodamine-labeled AG73-PEG liposomes (pDNA: 3 μg/mL) were added to the cells and incubated for 1 h at 37 °C. The cells were then collected, and the fluorescence intensities were measured by flow cytometry to evaluate the cellular association of liposomes.

To examine the effect of BLs and US exposure on cellular uptake of pDNA, AG73-PEG liposomes (encapsulated Cy3-labeled pDNA: 3 μg/mL) were added to cells and incubated for 4 h at 37 °C. After incubation, the cells were washed twice and BLs (120 μg/mL) were added. Then, US exposure was applied (frequency, 2028 kHz; duty, 50%; burst rate, 2.0 Hz; intensity, 1.0 W/cm^2; time, 10 s). Subsequently, the cells were incubated for 10 or 180 min, and then the cells were collected by trypsinization and washed with PBS supplemented with heparin (50 μg/mL) three times to remove AG73-PEG liposomes and pDNA bound to the cell surface. The fluorescence intensities were measured by flow cytometry.

Table 1. Characteristics of Prepared Liposomes[a]

	diameter (nm)	ζ-potential (mV)
nonlabeled PEG liposomes	155.6 ± 37.2	−4.77 ± 2.28
AG73-PEG liposomes	152.0 ± 17.2	−1.54 ± 0.25
AG73T-PEG liposomes	156.7 ± 38.5	−1.38 ± 0.33

[a] Data represent means and SD of three different determinations.

Confocal Laser Scanning Microscopy (CLSM). 293T-Syn2 cells (7×10^4) were seeded two days before the experiments. The cells were treated with AG73-PEG liposomes (Cy3-labeled pDNA: 3 μg/mL) and Alexa Fluor 488-conjugated transferrin (50 μg/mL) for 4 h at 37 °C. After incubation, the cells were washed and BLs (120 μg/mL) were added. Then, US exposure was applied (frequency, 2028 kHz; duty, 50%; burst rate, 2.0 Hz; intensity, 1.0 W/cm^2; time, 10 s). Subsequently, the cells were incubated for 10, 60, or 180 min and then fixed with 4% paraformaldehyde for 1 h at 4 °C. Then, CLSM was performed. To differentiate the AG73-PEG liposomes internalized into the cytoplasm following attachment to the surface of the cell membrane, the cytoplasm was distinguished from the cell membrane as shown in a previous paper.[39,40] The rate of colocalization of Cy3-labeled pDNA with Alexa Fluor 488-conjugated transferrin was quantified as follows: amount of colocalization (%) = Cy3 $\text{pixels}_{\text{colocalization}}$/Cy3 $\text{pixels}_{\text{total}} \times 100$, where Cy3 $\text{pixels}_{\text{colocalization}}$ represents the number of Cy3 pixels colocalizing with Alexa Fluor 488-conjugated transferrin and Cy3 $\text{pixels}_{\text{total}}$ represents the number of all Cy3 pixels.

Results

Characteristics of AG73-PEG Liposomes. We evaluated the average size and zeta potential of nonlabeled, AG73, or AG73T-PEG liposomes with 5 mol % DSPE-PEG_{2000} and modified with 3 mol % peptides. The size and zeta potential of the liposomes were determined as about 150 nm with a slight negative charge (Table 1).

Receptor-Mediated Gene Delivery by AG73-PEG Liposomes. We evaluated the selective association of AG73-PEG liposomes with 293T-Syn2 cells (Syndecan-2 overexpressing cell) via the syndecan-2 receptor. The cells were incubated with either nonlabeled, AG73, or AG73T-PEG liposomes containing Rhodamine-DOPE for 1 h at 37 °C, and fluorescence intensities were examined by flow cytom-

(39) Suh, J.; Wirtz, D.; Hanes, J. Efficient active transport of gene nanocarriers to the cell nucleus. Proc. *Natl. Acad. Sci. U.S.A.* **2003**, *100*, 3878–3882.

(40) Oba, M.; Aoyagi, K.; Miyata, K.; Matsumoto, Y.; Itaka, K.; Nishiyama, N.; Yamasaki, Y.; Koyama, H.; Kataoka, K. Polyplex micelles with cyclic RGD peptide ligands and disulfide cross-links directing to the enhanced transfection via controlled intracellular trafficking. *Mol. Pharmaceutics* **2008**, *5*, 1080–1092.

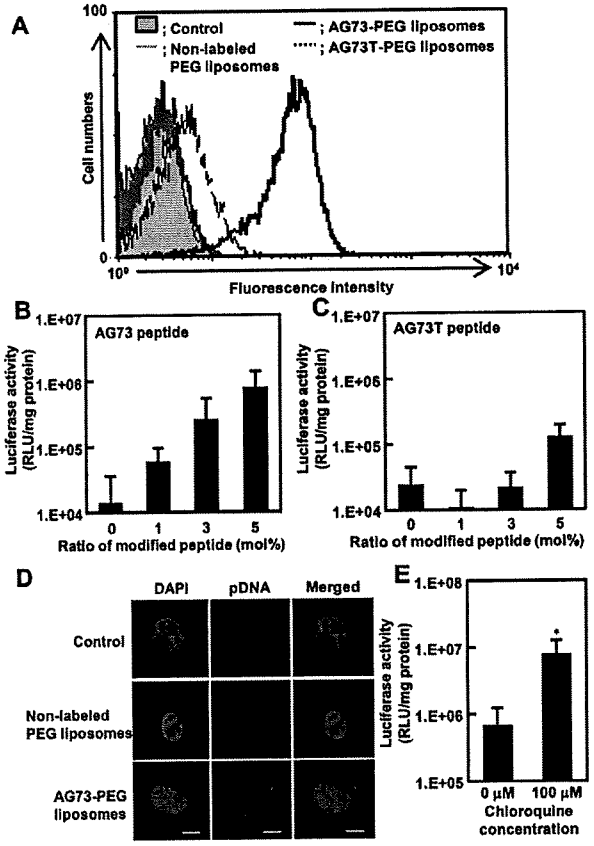

Figure 1. Effect of AG73 coating on liposome cell binding and gene transfer. (A) 293T-Syn2 cells were treated with either Rhodamine-labeled nonlabeled, AG73- or AG73T-PEG liposomes for 1 h at 37 °C. The fluorescence intensities were measured by flow cytometry. (B, C) The cells were incubated with the PEG liposomes modified with AG73 or AG73T in various ratios for 4 h at 37 °C. After replacement with fresh medium, the cells were cultured for 20 h and then luciferase activity was determined. Data are shown as means ± SD (n = 4). (D) The cells were treated with nonlabeled or AG73-PEG liposomes encapsulating Cy3-labeled pDNA (red) for 1 h at 37 °C. The nucleus was stained with DAPI (blue), and then the cells were observed by CLSM. The scale bars represent 10 μm. (E) The cells were preincubated with or without chloroquine for 30 min before transfection and then treated with AG73-PEG liposomes in the presence or absence of chloroquine for a further 4 h at 37 °C. After replacement with fresh medium, the cells were cultured for 20 h and luciferase activity was determined. Data are shown as means ± SD (n = 4). $^*p < 0.05$ compared with treatment in the absence of chloroquine.

etry. The cells treated with AG73-PEG liposomes showed an enhancement of fluorescence intensities compared with nonlabeled and AG73T-PEG liposomes (Figure 1A). The delivery efficiency of AG73-PEG liposomes was higher than that of the nonlabeled liposomes. Next, the effects of AG73 coating of PEG liposomes on gene transfection were examined. The cells were treated with AG73-PEG liposomes that were modified with AG73 at various ratios for 4 h at 37 °C, and then luciferase activity was measured after an additional incubation for 20 h. The increase in luciferase activity depended upon the ratio of AG73 modified with PEG liposomes, while the luciferase activity was not enhanced by AG73T-PEG liposomes (Figure 1B,C). Furthermore, to elucidate the subcellular localization of pDNA after uptake by syndecan-2 receptors, AG73-PEG liposomes containing Cy3-labeled pDNA were monitored in the cells by confocal laser scanning microscopy. In the cells treated with AG73-PEG liposomes, the fluorescence of pDNA was observed on the surface of the cell membrane and in the cytoplasm after incubation for 1 h. In contrast, the fluorescence of pDNA was weak in the cytoplasm of cells treated with nonlabeled PEG liposomes after a 1 h incubation (Figure 1D).

Although AG73-PEG liposomes could introduce genes into the cells via syndecan-2, it is believed that PEG-modification of liposomes affects the endosomal escape of liposomes, leading to a decrease in gene expression after transfection.[19−23] Therefore, to assess the ability for endosomal escape of AG73-PEG liposomes, cells were transfected with AG73-PEG liposomes in the presence of chloroquine, which is recognized as an endosomolytic agent.[41−43] The resulting luciferase activity was 10-fold higher than that following treatment with AG73-PEG liposomes in the absence of chloroquine (Figure 1E). We conclude that AG73-PEG liposomes can selectively deliver genes to the cells via syndecan-2, but they may not release genes into cytoplasm and nucleus efficiently.

Enhancement of AG73-Mediated Liposomal Gene Transfection by BLs and US. To investigate the effect of BLs and US exposure on the transfection efficiency of AG73-PEG liposomes, 293T-Syn2 cells were treated with either nonlabeled or AG73-PEG liposomes for 4 h at 37 °C in serum-free medium, and then the cells were treated with BLs and US exposure. After treatment with AG73-PEG liposomes, the luciferase activity was enhanced up to 60-fold by BLs and US exposure when compared with that of AG73-PEG liposomes alone. Furthermore, the combination of AG73-PEG liposomes with BLs and US exposure had about 60-fold higher luciferase activity than that of nonlabeled liposomes with BLs and US exposure (Figure 2A). We also examined the transfection efficiency by treatment of AG73-PEG liposomes with US in the absence of BLs. As a result,

(41) Wibo, M.; Poole, B. Protein degradation in cultured cells. II. The uptake of chloroquine by rat fibroblasts and the inhibition of cellular protein degradation and cathepsin B1. *J. Cell Biol.* **1974**, *63*, 430–440.

(42) Sonawane, N. D.; Szoka, F. C.; Verkman, A. S. Chloride accumulation and swelling in endosomes enhances DNA transfer by polyamine-DNA polyplexes. *J. Biol. Chem.* **2003**, *278*, 44826–44831.

(43) Cheng, J.; Zeidan, R.; Mishra, S.; Liu, A.; Pun, S. H.; Kulkarni, R. P.; Jensen, G. S.; Bellocq, N. C.; Davis, M. E. Structure-function correlation of chloroquine and analogues as transgene expression enhancers in nonviral gene delivery. *J. Med. Chem.* **2006**, *49*, 6522–6531.

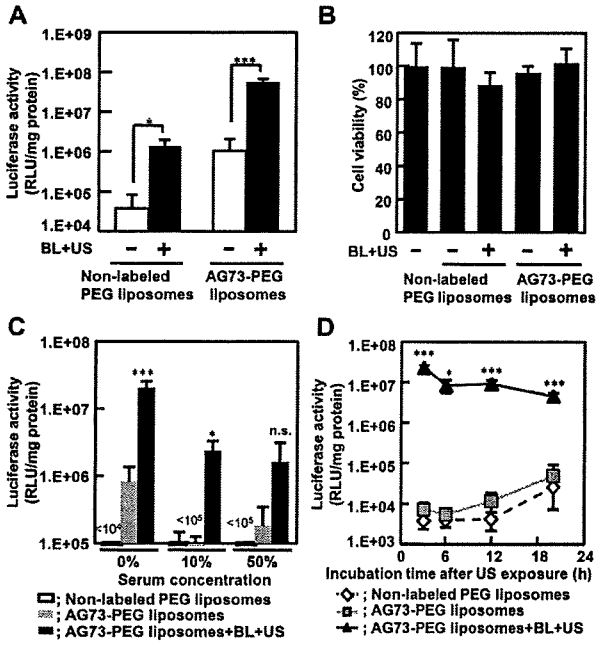

Figure 2. Effect of BLs and US exposure on AG73-mediated liposome-mediated gene transfection. (A, B) Nonlabeled or AG73-PEG liposomes were added to 293T-Syn2 cells. After 4 h incubation, the cells were washed and BLs were added. Then, the cells were exposed to US and cultured for 20 h. Then luciferase activity was determined and cell viability was measured using a MTT assay. Data are shown as means ± SD ($n = 4$). $^*p < 0.05$, $^{***}p < 0.005$. (C) The cells were treated with either nonlabeled or AG73-PEG liposomes in the various serum concentrations. After the incubation for 4 h, the cells were washed and BLs were added. Then, the cells were exposed to US and cultured for 20 h. Then, luciferase activity was determined. Data are shown as means ± SD ($n = 4$). $^*p < 0.05$, $^{***}p < 0.005$ compared with AG73-PEG liposomes. (D) Cells were treated with either nonlabeled or AG73-PEG liposomes. After incubation for 4 h, the cells were washed and BLs were added. Then, the cells were exposed to US and incubated for 3, 6, 12, or 20 h. Then, luciferase activity was determined. Data are shown as means ± SD ($n = 4$). $^*p < 0.05$, $^{***}p < 0.005$ compared with AG73-PEG liposomes.

the transfection efficiency was barely enhanced by treatment with AG73-PEG liposomes with US compared with that of AG73-PEG liposomes alone (data not shown). The cytotoxicity of the combination of AG73-PEG liposomes with BLs and US exposure was determined using an MTT assay. Cell viability was more than 90% even after each transfection (Figure 2B). Since cancer gene therapy in the clinic needs to be effective in the presence of serum, we examined the effects of serum on gene transfection by AG73-PEG liposomes with BLs and US exposure. As shown in Figure 2C, the luciferase activity after treatment with AG73-PEG liposomes was increased by BLs and US exposure even in the presence of serum.

The mechanism of transfection involving the combination of AG73-PEG liposomes with BLs and US exposure could be different from that of AG73-PEG liposomes alone. Therefore, to investigate the kinetics of gene expression, cells were treated with either nonlabeled or AG73-PEG liposomes for 4 h, and then the cells were treated with BLs and US exposure. Luciferase activity was measured sequentially after US exposure. As shown in Figure 2D, the luciferase activity after the treatment with AG73-PEG liposomes was enhanced by BLs and US exposure within 3 h after US exposure compared with that of nonlabeled or AG73-PEG liposomes alone. However, the luciferase activity after the treatment with either nonlabeled or AG73-PEG liposomes alone increased in a time-dependent manner; and the luciferase activity with the combination of AG73-PEG liposomes with BLs and US exposure was maintained at a higher level at all time points. We conclude that BLs and US exposure can enhance AG73 mediated liposomal gene transfection.

The Mechanism of Transfection by AG73-PEG Liposomes with BLs and US Exposure. To evaluate the effects of BLs and US exposure on the cellular uptake of pDNA, flow cytometry analysis was performed to measure the fluorescence intensities of Cy3-labeled pDNA in 293T-Syn2 cells transfected with AG73-PEG liposomes with or without BLs and US exposure. Cellular uptake of pDNA showed almost no difference in the presence of AG73-PEG liposomes with or without BLs and US exposure (Figure 3A). To examine the involvement of endocytosis in the process, the cells were first treated with AG73-PEG liposomes for 1 h at 37 °C or at 4 °C, and then the fluorescence intensity was measured by flow cytometry. As shown in Figure 3B, the fluorescence intensities of the cells treated with AG73-PEG liposomes for 1 h at 4 °C were decreased compared with the treatment of AG73-PEG liposomes for 1 h at 37 °C. Next, the involvement of endocytosis in the transfection with AG73-PEG liposomes was examined. The cells were transfected by AG73-PEG liposomes with or without BLs and US exposure at 37 or 4 °C. Twenty-three hours after transfection, the luciferase activity was measured. When the cells were transfected by AG73-PEG liposomes with BLs and US exposure at 37 °C, the luciferase activity was increased compared with that of the cells treated with AG73-PEG liposomes alone. In contrast, the luciferase activity did not change in the cells treated with AG73-PEG liposomes with BLs and US exposure at 4 °C compared with the treatment of AG73-PEG liposomes alone (Figure 3C).

We further established whether BLs and US exposure could enhance gene expression with AG73-PEG liposomes. The cells were treated with AG73-PEG liposomes for 4 h at 37 °C, and then AG73-PEG liposomes attached to the surface of the cell membrane were removed with trypsin and heparin, followed by BLs and US exposure treatment. As a result, the luciferase activity was increased by BLs and US exposure even when AG73-PEG liposomes attached to the surface of the cell membrane were removed (Figure 3D). The effects of chloroquine on gene transfection by AG73-PEG liposomes with BLs and US exposure were also examined. The cells

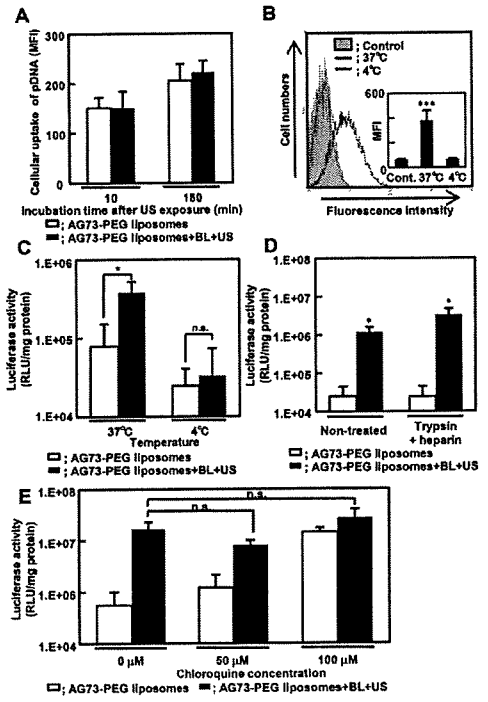

Figure 3. Mechanism of accelerated AG73-mediated liposomal gene transfer by BLs and US exposure. (A) 293T-Syn2 cells were incubated with AG73-PEG liposomes encapsulating Cy3-labeled pDNA for 4 h at 37 °C. After the incubation, the cells were washed and BLs were added. Then the cells were exposed to US and incubated for 10 or 180 min. Then, the cells were collected and washed with heparin-containing PBS three times. The fluorescence intensities were measured by flow cytometry. Data are shown as means ± SD ($n = 3$). (B) The cells were preincubated for 30 min at 37 or 4 °C before transfection and then treated with Rhodamine-labeled AG73-PEG liposomes for a further 1 h at 37 or 4 °C. The cells were then collected and washed with heparin-containing PBS three times. The fluorescence intensities were measured by flow cytometry. (C) The cells were preincubated for 30 min at either 37 or 4 °C before transfection and then treated with AG73-PEG liposomes for a further 1 h at 37 or 4 °C. After incubation, the cells were washed and BLs were added. Then, the cells were exposed to US and cultured for 23 h. Luciferase activity was determined. Data are shown as means ± SD ($n = 4$). *$p < 0.05$. (D) The cells were treated with AG73-PEG liposomes for 4 h at 37 °C and then washed with heparin-containing PBS following BLs and US exposure. The cells were cultured for 20 h and luciferase activity was determined. Data are shown as means ± SD ($n = 4$). *$p <$ 0.05 compared with AG73-PEG liposomes. (E) The cells were preincubated with or without chloroquine for 30 min before transfection and then treated with AG73-PEG liposomes in the presence or absence of chloroquine for a further 4 h. After incubation, the cells were washed and BLs were added. Then, the cells were exposed to US and cultured for 20 h. Then luciferase activity was determined. Data are shown as means ± SD ($n = 4$).

were pretreated for 30 min with chloroquine and transfected with pDNA using AG73-PEG liposomes with or without BLs and US exposure in the presence of chloroquine. As shown in Figure 3E, the cells treated with AG73-PEG liposomes alone showed the enhancement of luciferase activity in the presence of chloroquine (0−100 μM). In contrast, for cells treated using AG73-PEG liposomes with BLs and US exposure, the luciferase activity was not affected significantly even at the high dose of chloroquine. We conclude that BLs and US exposure can affect AG73-PEG liposomes internalized into the cells.

Intracellular Distribution of pDNA. To evaluate the intracellular distribution of pDNA, 293T-Syn2 cells were treated with AG73-PEG liposomes containing Cy3-labeled pDNA in the presence of Alexa Fluor 488-conjugated transferrin for 4 h, and then the cells were treated with BLs and US exposure. After the US exposure, cells were incubated for 10, 60, or 180 min and observed by confocal laser scanning microscopy. In the cells treated with AG73-PEG liposomes alone, the fluorescence of pDNA colocalized with the fluorescence of transferrin (Figure 4A). In contrast, the fluorescence of pDNA colocalized with transferrin was reduced. The ratio of Cy3-labeled pDNA with Alexa Fluor 488-conjugated transferrin was also quantified. As shown in Figure 4B, the ratio of colocalization of Cy-3 labeled pDNA with Alexa Fluor 488-conjugated transferrin was decreased by treatment with AG73-PEG liposomes with BLs and US exposure compared with the treatment of AG73-PEG liposomes alone. We conclude that BLs and US exposure can affect the intracellular trafficking of pDNA and enhance the transfection efficacy of AG73-PEG liposomes.

Discussion

The selective delivery of pDNA into tumors could enhance cancer gene therapy, and some targeting of ligands, such as transferrin, folate, anisamide, RGD-peptides, and antibodies, has been used.[5−10] For selective gene delivery into tumors, AG73-PEG liposomes encapsulating pDNA were developed. The laminin-derived AG73 peptide is a known ligand for syndecans, and it has been reported that syndecan-2 is highly expressed in various cancer cells.[11−13,15,17]

First, it was assessed whether the AG73-PEG liposomes could deliver genes to syndecan-2-overexpressing cancer cells (293T-Syn2 cells) selectively. The cellular association (Figure 1A), transfection efficacy (Figure 1B,C), and cellular uptake (Figure 1D) were examined. AG73-PEG liposomes could strongly associate with 293T-Syn2 cells, deliver pDNA effectively into the cells, and increase luciferase gene expression depending upon the ratio of AG73 peptide modified PEG liposomes used. These results suggested that AG73 is involved in the association of the liposomes with the cells via Syndecan2, and that pDNA can be internalized efficiently into cells, leading to the increase in gene expression.

PEG-modification is believed to suppress cellular association and/or endosomal escape of liposomes, and it decreased

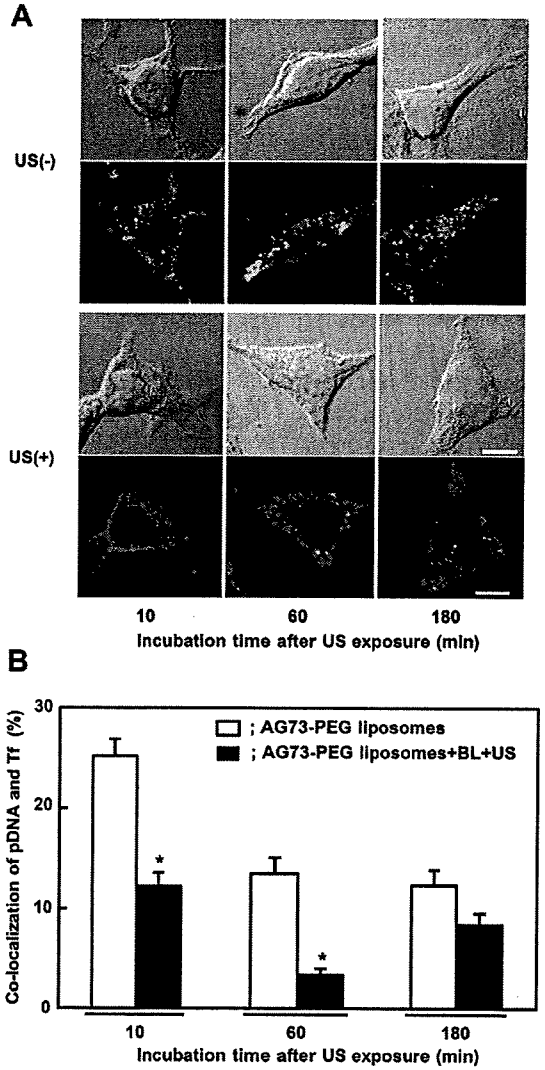

Figure 4. Effect of BLs and US exposure on the colocalization of pDNA and transferrin. (A, B) 293T-Syn2 cells were treated with AG73-PEG liposomes encapsulating Cy3-labeled pDNA (red) and Alexa Fluor 488-conjugated transferrin (green) for 4 h at 37 °C. After incubation, the cells were washed and BLs were added. Then, the cells were exposed to US and incubated for 10, 60, or 180 min. Then the cells were fixed with 4% paraformaldehyde for 1 h at 4 °C and observed by CLSM. The scale bars represent 10 μm. The ratio of colocalization of Cy3-labeled pDNA with Alexa Fluor 488-conjugated transferrin was quantified. Data are shown as means ± SE (n = 100). *$p < 0.05$ compared with AG73-PEG liposomes (Mann–Whitney's U test).

gene expression.[19–23] Therefore, it was assessed whether AG73-PEG liposomes could transport pDNA into the cytoplasm and nucleus by escaping from endosomes efficiently. In the presence of chloroquine, the luciferase gene expression by AG73-PEG liposomes was apparently increased when compared with incubation without chloroquine (Figure 1D). This result suggested that AG73-PEG liposomes may not deliver the encapsulated pDNA into the cytoplasm and nucleus efficiently. It was also confirmed that AG73-liposomes without PEG modification generated higher gene expression when compared with AG73-PEG liposomes (data not shown). However, it was necessary to stabilize liposomes in the blood to obtain therapeutic efficacy in systemic cancer gene therapy. Therefore, it is necessary to further enhance the transfection efficacy by PEG-modified liposomes for cancer gene therapy *in vivo*.

The present study developed echo-contrast gas entrapping liposomes (BLs) and found that BLs and US exposure could enhance the permeability of tissue cell membranes transiently.[35–38] It was also hypothesized that BLs and US might affect not only the cell membrane but also intracellular vesicles and enhance the escape of pDNA from endosomes into the cytoplasm. We assessed whether AG73-mediated liposomal gene transfection could be enhanced by BLs and US exposure. To determine the effects of BLs and US exposure on AG73-PEG liposomes either within the cells or attached to the surface of the cell membrane, excess AG73-PEG liposomes in the medium were removed after a 4 h incubation. Gene transfection efficiency with AG73-PEG liposomes was enhanced by BLs and US exposure even in the presence of serum (Figure 2A,C), and higher luciferase gene expression was observed at 3 h after US exposure compared with treatment with AG73-PEG liposomes alone (Figure 2D). It was shown that luciferase expression remained at a plateau, rather than decreasing, following treatment using AG73-PEG liposomes with BLs and US exposure (Figure 2D). For this reason, it may be considered that pDNA/poly-L-lysine complexes may be first decondensed and the naked pDNA may be degraded gradually after treatment with BLs and US exposure, which could affect the intracellular trafficking of pDNA leading to enhancement of the release of pDNA from endosomes into the cytosol and the transfer of pDNA to the nucleus. Therefore, luciferase expression could increase at an early time point and then decrease in a time-dependent manner. In contrast, in treatments with AG73-PEG liposomes or nonlabeled PEG liposomes alone, luciferase expression increased (Figure 2D). For this reason, it may be considered that AG73-PEG liposomes attached to the cell membrane via syndecan-2 or nonlabeled PEG liposomes attached to the cell membrane nonspecifically, which could not be removed completely and might be internalized in a time-dependent manner, leading to a gradual increase in luciferase expression subsequently. We also confirmed an enhancement of the transfection efficiency of AG73-PEG liposomes by BLs and US exposure in B16 melanoma cells expressing syndecan-2 (data not shown). These results suggest that BLs and US exposure can lead to enhanced gene expression.

We determined the mechanism of the enhancement of AG73-mediated liposomal gene transfection by BLs and US exposure. It had been speculated that BLs and US exposure could affect cell membranes and/or intracellular vesicles and enhance the intracellular transport of AG73-PEG liposomes

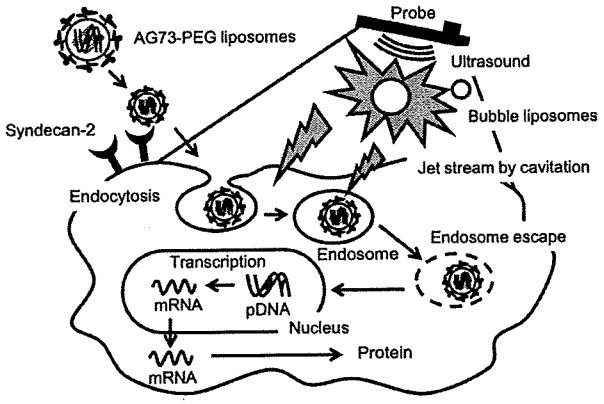

Figure 5. Diagram of gene transfer by AG73-PEG liposomes with Bubble liposomes and ultrasound exposure.

and the trafficking of AG73-PEG liposomes. Therefore, the effect of BLs and US exposure on cellular internalization of pDNA was investigated by flow cytometry (Figure 3A). However, the fluorescence intensities of pDNA in the cells were not affected remarkably by BLs and US exposure. Next, it was examined whether BLs and US exposure could affect AG73-PEG liposomes either attached to the surface of the cell membrane or internalized into cells. The uptake of AG73-PEG liposomes into the cells was diminished at 4 °C. The transfection efficiency by itself was not enhanced significantly by BLs and US exposure at 4 °C. In contrast, luciferase activity was increased when BLs and US exposure were applied to the cells internalizing AG73-PEG liposomes (Figure 3B–D). In addition, although the transfection efficiency of AG73-PEG liposomes alone was enhanced in the presence of chloroquine, the transfection efficiency of AG73-PEG liposomes with BLs and US exposure was not increased significantly (Figure 3E). These results suggested that BLs and US exposure could affect AG73-PEG liposomes internalized into the cells but did not affect AG73-PEG liposomes attached to the surface of the cell membrane and could present effects such as chloroquine (Figure 5). It may be possible that BLs and US exposure affect RNA transcription, but this seems unlikely because further increases in gene expression were not observed with the enhanced endosomal escape by chloroquine (Figure 3D). Furthermore, the intracellular distribution of pDNA was observed. The ratio of colocalization of pDNA and transferrin was decreased by treatment with BLs and US exposure (Figure 4). This result suggested that BLs and US exposure could affect the intracellular trafficking of pDNA and increase the transfection efficacy of AG73-PEG liposomes (Figure 5). It has been reported that microbubble and US exposure could directly deliver lipoplex into the cytoplasm of the cell.[44] However, we suggested that AG73-PEG liposomes could not significantly enter into cytoplasm directly by the treatment of BLs and US exposure (Figure 3C). Therefore, there is a possibility that AG73-PEG liposomes associated with syndecan-2 receptor of the cells might not directly enter into cytoplasm by the treatment of BLs and US exposure.

However, we should elucidate a more particular mechanism by which BLs and US exposure may affect directly intracellular vesicle morphology or induce several biological effects such as influx of calcium ions or generation of reactive oxygen species,[45–48] but that has not yet been determined.

In conclusion, it was shown that PEG liposomes modified with AG73 peptide, which is a ligand for syndecans, could be a useful vector for syndecan-2 overexpressing cancer cells. In addition, the combination of BLs and US exposure could enhance AG73-mediated liposomal gene transfection. BLs and US exposure could not promote the transportation of AG73-PEG liposomes into cells but did affect the intracellular trafficking of AG73-PEG liposomes, leading to an increase in gene expression. BLs and US exposure may overcome the disadvantages of PEG-modified liposomes and enhance the delivery efficiency of genes into the cytoplasm and nucleus. Thus, the combination of AG73-PEG liposomes with BLs and US exposure may be a promising method to achieve selective and efficient gene delivery for cancer gene therapy via systemic administration.

Abbreviations Used

PEG, polyethyleneglycol; BLs, Bubble liposomes; US, ultrasound; pDNA, plasmid DNA; DOPE, 1;2-dioleoyl-*sn*-glycero-3-phosphoethanolamine; DOPG, 1,2-dioleoyl-*sn*-glycero-3-phospho-*rac*-1-glycerol; DSPE, 1,2-distearoyl-*sn*-glycero-3-phosphatidylethanolamine; Mal, maleimide; Fmoc, fluorenylmethoxycarbonyl; FBS, fetal bovine serum; PLL, poly-L-lysine.

Acknowledgment. We are grateful to Dr. Katsuro Tachibana (Department of Anatomy, School of Medicine, Fukuoka University) for technical advice regarding the induction of cavitation with US, and to Mr. Yasuhiko Hayakawa, Mr. Takahiro Yamauchi, and Mr. Kosho Suzuki

(44) Lentacher, I.; Wang, N.; Vandenbroucke, R. E.; Demeester, J.; De Smedt, S. C.; Sander, N. N. Ultrasound exposure of lipoplex loaded microbubbles facilitates direct cytoplasmic entry of the lipoplexes. *Mol. Pharmaceutics* **2009**, *6*, 457–467.

(45) Juffermans, L. J.; Dijkmans, P. A.; Musters, R. J.; Visser, C. A.; Kamp, O. Transient permeabilization of cell membranes by ultrasound-exposed microbubbles is related to formation of hydrogen peroxide. *Am. J. Physiol.* **2006**, *291*, H1595–H1601.

(46) Juffermans, L. J.; Kamp, O.; Dijkmans, P. A.; Visser, C. A.; Musters, R. J. Low-intensity ultrasound-exposed microbubbles provoke local hyperpolarization of the cell membrane via activation of BK(Ca) channels. *Ultrasound Med. Biol.* **2008**, *34*, 502–508.

(47) Zhou, Y.; Shi, J.; Cui, J.; Deng, C. X. Effects of extracellular calcium on cell membrane resealing in sonoporation. *J. Controlled Release* **2008**, *126*, 34–43.

(48) Kumon, R. E.; Aehle, M.; Sabens, D.; Parikh, P.; Han, Y. W.; Kourennyi, D.; Deng, C. X. Spatiotemporal effects of sonoporation measured by real-time calcium imaging. *Ultrasound Med. Biol.* **2009**, *35*, 494–506.

(NEPA GENE CO., LTD.) for technical advice regarding exposure to US. This study was supported by an Industrial Technology Research Grant (04A05010) from the New Energy and Industrial Technology Development Organization (NEDO) of Japan, Grant-in-aid for Exploratory Research (18650146) and Grant-in-aid for Scientific Research (B) (20300179) from the Japan Society for the Promotion of Science, and by a grant for private universities provided by the Promotion and Mutual Aid Corporation for Private Schools of Japan.

MP900214S

Journal of Controlled Release 142 (2010) 245–250

Contents lists available at ScienceDirect

Journal of Controlled Release

journal homepage: www.elsevier.com/locate/jconrel

Cancer gene therapy by IL-12 gene delivery using liposomal bubbles and tumoral ultrasound exposure

Ryo Suzuki [a,1], Eisuke Namai [a,1], Yusuke Oda [a,1], Norihito Nishiie [a], Shota Otake [a], Risa Koshima [a], Keiichi Hirata [a], Yuichiro Taira [a], Naoki Utoguchi [a], Yoichi Negishi [b], Shinsaku Nakagawa [c], Kazuo Maruyama [a,*]

[a] Department of Biopharmaceutics, School of Pharmaceutical Sciences, Teikyo University, Sagamihara, Kanagawa, Japan
[b] Department of Drug and Gene Delivery System, School of Pharmacy, Tokyo University of Pharmacy and Life Science, Hachioji, Tokyo, Japan
[c] Department of Biotechnology and Therapeutics, Graduate School of Pharmaceutical Sciences, Osaka University, Suita, Osaka, Japan

ARTICLE INFO

Article history:
Received 24 August 2009
Accepted 26 October 2009
Available online 31 October 2009

Keywords:
Interleukin-12 (IL-12)
Ultrasound
Liposomes
Cancer gene therapy
Non-viral vector

ABSTRACT

Interleukin-12 (IL-12) gene therapy is expected to be effective against cancers because it primes the immune system for cancer cells. In this therapy, it is important to induce IL-12 gene expression in the tumor tissue. Sonoporation is an attractive technique for developing non-invasive and non-viral gene delivery systems, but simple sonoporation using only ultrasound is not an effective cancer gene therapy because of the low efficiency of gene delivery. We addressed this problem by combining ultrasound and novel ultrasound-sensitive liposomes (Bubble liposomes) which contain the ultrasound imaging gas perfluoropropane. Our previous work showed that this is an effective gene delivery system, and that Bubble liposome collapse (cavitation) is induced by ultrasound exposure. In this study, we assessed the utility of this system in cancer gene therapy using IL-12 corded plasmid DNA. The combination of Bubble liposomes and ultrasound dramatically suppressed tumor growth. This therapeutic effect was T-cell dependent, requiring mainly $CD8^+$ T lymphocytes in the effector phase, as confirmed by a mouse *in vivo* depletion assay. In addition, migration of $CD8^+$ T cells was observed in the mice, indicating that the combination of Bubble liposomes and ultrasound is a good non-viral vector system in IL-12 cancer gene therapy.

1. Introduction

Interleukin 12 (IL-12), a heterodimeric protein composed of p35 and p40 subunits [1,2], is produced by antigen-presenting cells such as dendritic cells and macrophages. IL-12 has a variety of immunomodulatory anti-tumor effects including induction of interferon-γ (IFN-γ secretion by stimulation of T cells and natural killer (NK) cells, and promotion of cytotoxic T lymphocyte (CTL) maturation [3,4]. In addition, IL-12 induces antiangiogenic effects mainly through IFN-γ-dependent production of the chemokine, interferon-inducible protein-10 (IP-10) [5], suggesting that IL-12 would be an effective anti-tumor agent. Although the systemic administration of IL-12 has been shown to suppress tumor growth, clinical trials were interrupted because of fatal adverse effects [6,7]. On the other hand, local administration of IL-12 into tumors is accepted as a more effective immunotherapeutic approach because of reduced systemic toxicity [8]. In particular, gene therapy by intratumoral injection of the IL-12 gene is expected to be an effective cancer therapy because it would lead to the locally sustained release of IL-12 in the tumor [9].

In cancer gene therapy, it is important to develop easy, safe, efficient and minimally-invasive techniques for transferring genes into tumor tissue. Non-viral gene therapy has many advantages over gene therapy, including ease of plasmid DNA production, lower toxicity and immunogenicity, and lower cost. Many researchers have attempted to develop non-viral gene delivery carriers such as lipids and polymers [10–13]. In addition, there is wide interest in the potential of therapeutic ultrasound for enhancing the efficiency of gene delivery [14,15]. In particular, a physical method using ultrasound combined with nano/microbubbles has many of the desired characteristics for an ideal gene therapy, including low toxicity, the potential for repeated applications, organ specificity, and broad applicability to acoustically accessible organs [16,17]. Ultrasound can create transient nonlethal perforations in cell membranes [18], allowing extracellular plasmid DNA to be directly delivered into the cytosol. The main mechanism of gene delivery is thought to be acoustic cavitation using nano/microbubbles as cavitation nuclei. Based on liposome technology, we previously developed novel liposomal bubbles (Bubble liposomes) containing lipid micelles of the ultrasound imaging gas, perfluoropropane [19–23]. When coupled with ultrasound exposure, Bubble liposomes could

* Corresponding author. 1091-1 Suwarashi, Sagamiko, Sagamihara, Kanagawa 229-0195, Japan. Tel.: +81 42 685 3724; fax: +81 42 685 3432.
E-mail address: maruyama@pharm.teikyo-u.ac.jp (K. Maruyama).
[1] The first three authors contributed equally to this work.

0168-3659/$ – see front matter © 2009 Elsevier B.V. All rights reserved.
doi:10.1016/j.jconrel.2009.10.027

be used as novel gene delivery agents *in vitro* and *in vivo* [19,20,24]. In addition, we found that gene delivery into femoral artery with this method was much more efficient than the conventional lipofection method using Lipofectamine 2000 [19]. And there is little report about cancer gene therapy using nano/microbubbles and ultrasound. Therefore, it is expected that gene delivery using Bubble liposomes and ultrasound will be an effective non-viral vector system for cancer gene therapy. In this study, we assessed this gene delivery system in cancer gene therapy using IL-12 gene.

2. Materials and methods

2.1. Cells and animals

Murine ovarian carcinoma OV-HM cells were kindly provided by Dr. Hiromi Fujiwara. An ovarian tumor OV2944, was induced in a female (C57BL/6 X C3H/He) F_1 mice by giving a single whole-body neutron irradiation, and a cloned line with highly metastatic property (designated OV-HM) was isolated from the parental line [25]. OV-HM cells were grown in RPMI-1640 (Sigma Chemical Co., St. Louis, MO) containing 100 U/ml penicillin (Wako Pure Chemical Industries, Osaka, Japan) and 100 μg/ml streptomycin (Wako Pure Chemical Industries) supplemented with 10% heat-inactivated fetal bovine serum (FBS, GIBCO, Invitrogen Co., Carlsbad, CA). B6C3F1 female mice were obtained from Sankyo Labo Service Corporation, Inc. (Tokyo, Japan) and used at 6 weeks of age. All of the experimental procedures were performed in accordance with the Teikyo University guidelines for the welfare of animals in studies of experimental neoplasia.

2.2. Preparation of Bubble liposomes

Liposomes composed of 1,2-distearoyl-sn-glycero-phosphatidylcholine (DSPC) (NOF Corp., Tokyo, Japan) and 1,2-distearoyl-sn-glycero-3-phosphatidyl-ethanolamine s-methoxypolyethyleneglycol (DSPE-PEG(2 k)-OMe, (PEG, Mw = ca. 2000); NOF) (94:6 (m/m)) were prepared by reverse phase evaporation. Briefly, all reagents (total lipid: 100 μmol) were dissolved in 8 ml of 1:1 (v/v) chloroform/diisopropyl ether, and then 4 ml of phosphate buffered saline (PBS) was added. The mixture was sonicated and evaporated at 65 °C. The organic solvent was completely removed, and the size of the liposomes was adjusted to less than 200 nm using an extruding apparatus (Northern Lipids Inc., Vancouver, Canada) and sizing filters (pore sizes: 100 and 200 nm; Nuclepore Track-Etch Membrane, Whatman plc, UK). After sizing, the liposomes were sterilized by passing them through a 0.45-μm pore size filter (Millex HV filter unit, Durapore PVDF membrane, Millipore Corp., MA). The size of the liposomes was measured by dynamic light scattering (ELS-800, Otsuka Electronics Co., Ltd., Osaka, Japan). The average diameter of these liposomes was between 150 and 200 nm. Lipid concentration was measured using the Phospholipid C test (Wako Pure Chemical Industries). Bubble liposomes were prepared from the liposomes and perfluoropropane gas (Takachiho Chemical Industrial Co., Ltd., Tokyo, Japan). Briefly, 5-ml sterilized vials containing 2 ml of the liposome suspension (lipid concentration: 2 mg/ml) were filled with perfluoropropane, capped, and then supercharged with 7.5 ml of perfluoropropane. The vial was placed in a bath-type sonicator (42 kHz, 100 W; Bransonic 2510 J-DTH, Branson Ultrasonics Co., Danbury, CT) for 5 min to form the Bubble liposomes. In this method, the liposomes were reconstituted by sonication and supercharged with perfluoropropane in the 5-mL vial container. Perfluoropropane was entrapped within the lipid micelles, comprising DSPC and DSPE-PEG (2 k)-OMe, to form nanobubbles. The lipid nanobubbles were encapsulated within the reconstituted liposomes, which now ranged in size from around 500 nm–1 μm, compared to 150–200 nm before supercharging with perfluoproropane.

2.3. Plasmid DNA vector construction

The plasmid pCMV-Luc contained the firefly luciferase gene of pGL3-control (Promega) at the *HindIII/XbaI* site of the pcDNA3 vector (Invitrogen). This plasmid was an expression vector encoding the firefly luciferase gene under the control of a cytomegalovirus promoter. The plasmid pCMV-IL12 contained murine IL-12, derived from mIL-12 BIA/pBluescript II KS(−) (kindly provided by Dr. Yamamoto, Department of Immunology, Graduate School of Pharmaceutical Sciences, Osaka University, Japan) in the *XhoI/NotI* site of the pHMCMV5 vector. This expression vector encoded the murine IL-12 gene under the control of a cytomegalovirus promoter [26].

2.4. Intratumoral administration of plasmid DNA

B6C3F1 mice were intradermally inoculated with OV-HM cells (1×10^6 cells/mouse) in the flank. After 7 days, a suspension (25 μL/mouse) of Bubble liposomes (2.5 μg) and pCMV-Luc or pCMV-IL12 (10 μg) was injected into the tumor, and ultrasound (1 MHz, 0.7 W/cm^2, 60 s) was transdermally applied to the tumor tissue. A conventional lipofection method was also investigated. A suspension (25 μL/mouse) of Lipofectamine 2000 (20 μg) and pCMV-Luc or pCMV-IL12 (10 μg) were incubated together for 20 min to allow them to complex. Then the complex was injected into the tumor. All treatment groups consisted of five mice.

2.5. Luciferase assay

Each day after the pCMV-Luc injection, mice were sacrificed and the tumor tissue was recovered. The tumor tissue was homogenized in lysis buffer (0.1% Triton X-100, 0.1 M Tris–HCl pH 7.8, 2 mM EDTA) and frozen (−80 °C) and thawed at room temperature twice. The homogenized tumor tissue was centrifuged (12,000 rpm, 4 °C, 10 min) and the supernatant was recovered for the luciferase assay. Luciferase activity was measured using a luciferase assay system (Promega) and luminometer (TD-20/20, Turner Designs, Sunnyvale, CA). The activity was measured as relative light units (RLU) per milligram protein.

2.6. Reverse transcription-polymerase chain reaction (RT-PCR) analysis for IL-12 expression in tumor tissues

OV-HM tumors were collected 1 or 2 days after intratumoral injection of pCMV-IL12 and Bubble liposomes, and total RNA was isolated using ISOGEN according to the manufacturer's instructions and dissolved with 20 μL TE buffer. RT proceeded for 60 min at 42 °C in 20 μl reaction mixture containing 1 μg total RNA treated with DNase I, 5 mM $MgCl_2$, RNA PCR buffer (Takara Bio, Kyoto, Japan), 1 mM dNTP mix, 0.125 μM Oligo dT-Adaptor primer (Takara Bio), 0.5 U/μL RNase inhibitor and 0.25 U/μL AMV reverse transcriptase XL (Takara Bio). PCR amplification of IL-12 and β-actin transcripts was performed in 20 μL reaction mixture containing 2 μL RT-material, PCR buffer, 0.5 U Takara Ex Taq HS, 0.2 mM dNTP, 2.5 mM $MgCl_2$, and 0.4 mM primers. The sequences of the specific primers were as follows: murine IL-12: forward, 5′-ctc acc tgt gac acg cct ga-3′; reverse, 5′-cag gac act gaa tac ttc tc-3′; and murine β-actin: forward, 5′-tgt gat ggt ggg aat ggg tca g-3′; reverse, 5′-ttt gat gtc acg cac gat ttc c-3′. After denaturation for 5 min at 95 °C, three sequential steps, denaturation for 45 s at 95 °C, annealing for 60 s at 48 °C, and extension for 2 min at 72 °C, were repeated for 40 cycles, with a final extension step for 4 min at 72 °C.

EZ Load (Bio-Rad Laboratories, Inc., Tokyo, Japan) was used as a 100-bp molecular ladder. The PCR products were electrophoresed through a 2% agarose gel, stained with ethidium bromide, and visualized under ultraviolet radiation. The expected PCR product sizes were 430 bp (IL-12) and 514 bp (β-actin).

2.7. Anti-tumor effect of intratumoral administration on IL-12 gene expression in mice

B6C3F1 mice were intradermally inoculated with OV-HM cells (1×10^6 cells/mouse) into the flank. For single therapy, established tumors with diameters of 8–10 mm were injected with a suspension (25 μL/mouse) of Bubble liposomes (2.5 μg) and pCMV-IL12 (10 μg), and ultrasound (1 MHz, 0.7 W/cm^2, 60 s) was transdermally applied to the tumor tissue. We also examined the intratumoral injection of a complex (25 μL/mouse) of Lipofectamine 2000 (20 μg) and pCMV-IL12 (10 μg) as a conventional lipofection method for comparison. For repetitive therapy, the mice were treated as above on days 0, 2, 5, 7, 9 and 12 after first treatment. The anti-tumor effects were evaluated by measuring tumor volume. Tumor volume was calculated using the formula: (major axis × minor axis^2) × 0.5. All data are expressed as relative tumor volume to that before the first treatment. All treated groups contained five mice.

2.8. In vivo depletion analysis

GK1.5 hybridoma (rat anti-mouse CD4 mAb) and 53-6.72 hybridoma (rat anti-mouse CD8 mAb) were purchased from American Type Culture Collection (ATCC) (Manassas, VA). Ascites from BALB/c nude mice intraperitoneally injected with each hybridoma were collected, and antibodies were purified using a protein A column (GE Healthcare, Pollards Wood, UK). Mice bearing OV-HM were intratumorally injected with pCMV-IL12 and Bubble liposomes on days 0, 2, 5, 7, 9 and 12 after the first treatment. Additionally, the mice were intraperitoneally injected four times on days −3, 4, 11 and 18 after the first treatment with 100 μg/mouse of anti-mouse CD8 mAb for CD8$^+$ cells or anti-mouse CD4 antibody for CD4$^+$ cells, or on days −3, −2, −1, 0, 5, 10, 15 and 20 after the first treatment with 200 μg/mouse of anti asialoGM1 mAb (Wako Pure Chemical Industries) for NK cells. The depletion of T-cell subsets and NK cells was confirmed by flow cytometric analysis of peripheral blood. Tumor growth was monitored as described above.

2.9. Immunohistochemical analysis

B6C3F1 mice were intradermally inoculated with OV-HM cells (1×10^6 cells/mouse) into the flank. After 7, 9 or12 days, a suspension (25 μL/mouse) of Bubble liposomes (2.5 μg) and pCMV-IL12 (10 μg) was injected into the tumor, and ultrasound (1 MHz, 0.7 W/cm^2, 60 s) was transdermally applied to the tumor tissue. After 13 days of tumor inoculation, the mice were sacrificed, and the tumor tissue was dissected and then embedded in the OCT compound. Frozen sections (10 μm thick) were fixed with 4% paraformaldehyde at 4 °C for 10 min, and treated with 0.3% H_2O_2 in methanol:PBS (1:1) for 15 min and 1.5% normal cow serum in PBS for 10 min at room temperature. The sections were treated with rat anti-mouse CD8 mAbs (1:100) or rat anti-mouse perforin mAbs (1:100) (Kamiya Biomedical Co., Seattle, WA) in PBS containing 0.1% BSA at 4 °C overnight. The section was washed and treated with horse radish peroxidase-conjugated goat anti-rat IgG Abs (1:500) in PBS containing 0.1% BSA at room temperature for 2 h. The diaminobenzidine-reaction system (Vector Laboratories, Burlingame, CA) was used to stain the sections. We also stained the sections with hematoxylin solution for counterstaining. The samples were observed with a microscope (IX-71, Olympus, Tokyo, Japan).

2.10. Statistical analysis

Differences between experimental groups were compared with non-repeated measures ANOVA and Dunnett's test.

3. Results

3.1. Bubble liposomes and ultrasound-mediated gene delivery into solid tumors

To evaluate the effectiveness of gene delivery with Bubble liposomes and ultrasound into OV-HM solid tumors, we utilized the luciferase reporter gene expression assay (Fig. 1a). The effectiveness of gene delivery with conventional lipofection using Lipofectamine 2000 was also examined. Luciferase expression with ultrasound or Bubble liposomes was low, and even lower with Lipofectamine 2000. On the other hand, luciferase expression with the combination of Bubble liposomes and ultrasound exposure was higher than in the other groups. Therefore, the profile of luciferase expression was measured in mice treated with Bubble liposomes and ultrasound. Luciferase expression gradually decreased after transfection (Fig. 1b), with the elimination rate constant (Ke) and half period ($T_{1/2}$) of gene expression being 1.26 days^{-1} and 0.54 days, respectively.

3.2. IL-12 gene expression in solid tumors transfected with IL-12 corded plasmid DNA using Bubble liposomes and ultrasound

To assess IL-12 expression in solid tumors transfected with IL-12 corded plasmid DNA (pCMV-IL12), the expression of IL-12p40 mRNA was examined with RT-PCR (Fig. 2). No expression of IL-12p40 mRNA in solid tumors transfected with pCMV-IL12 was observed. A small amount of IL-12p40 mRNA was expressed in solid tumors transfected with pCMV-IL12 using Lipofectamine 2000 on 1 day after gene transfection. On the other hand, the expression of IL-12p40 mRNA was observed in solid tumors transfected with pCMV-IL12 using Bubble liposomes and ultrasound for at least 2 days after gene transfection. This result indicates that IL-12 is expressed more effectively in solid tumors transfected using Bubble liposomes and ultrasound than using Lipofectamine 2000.

3.3. Anti-tumor effect of IL-12 gene delivery with Bubble liposomes and ultrasound

First, we examined the effect of a single delivery of IL-12 gene (Fig. 3a). Gene delivery using Bubble liposomes, ultrasound or

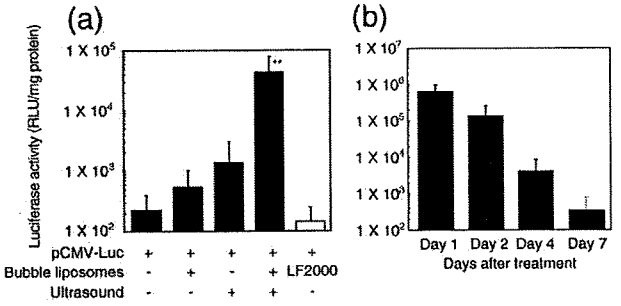

Fig. 1. Gene expression profiles in solid tumors following gene delivery with Bubble liposomes and ultrasound. Comparison of gene expression efficiency by gene delivery with each gene delivery method. B6C3F1 mice were intradermally inoculated with 1×10^6 OV-HM cells into the flank. Seven days after inoculation, the tumors were injected with pCMV-Luc (10 μg) using Bubble liposomes (2.5 μg) and/or ultrasound (1 MHz, 0.7 W/cm^2, 1 min), or Lipofectamine 2000 as a conventional lipofection method. (a) Two days after gene delivery, the mice were sacrificed and luciferase expression was measured in the solid tumor tissue. The data represent means ± SD ($n=3$). (b) Time course of luciferase expression after gene delivery with Bubble liposomes and ultrasound. Luciferase expression was measured at each time point after pCMV-Luc delivery into the solid tumor with Bubble liposomes and ultrasound exposure. $^{**}P<0.01$ compared to the group treated with plasmid DNA, Bubble liposomes, ultrasound or LF2000. LF2000: Lipofectamine 2000.

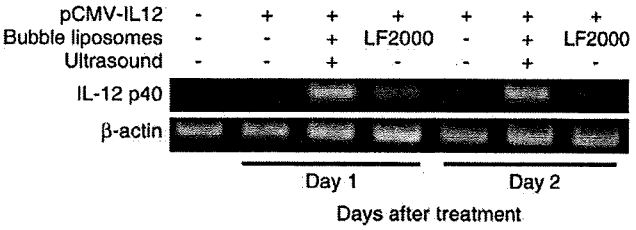

Fig. 2. RT-PCR analysis of IL-12 expression in solid tumors after pCMV-IL12 gene delivery. B6C3F1 mice were intradermally inoculated with 1×10^6 OV-HM cells into the flank. Seven days after inoculation, the tumors were injected with pCMV-IL12 (10 μg) using Bubble liposomes (2.5 μg) and/or ultrasound (1 MHz, 0.7 W/cm^2, 1 min), or Lipofectamine 2000 as a conventional lipofection method. One or 2 days after gene delivery, the mice were sacrificed, total RNA was prepared from the tumors, then RT-PCR was performed using a specific IL-12 primer as described in Materials and Methods. The PCR products were electrophoresed though a 3% agarose gel and stained with EtBr. To ensure the quality of the procedure, RT-PCR was performed on the same sample using a specific β-actin primer. LF2000: Lipofectamine 2000.

Lipofectamine 2000 showed no apparent anti-tumor effect, as was found for pCMV-Luc intratumoral delivery using Bubble liposomes and ultrasound. In contrast, the growth of OV-HM tumors was dramatically suppressed in mice treated by pCMV-IL12 intratumoral delivery using Bubble liposomes and ultrasound; however, complete regression was not observed. Thus, we examined the effect of repetitive IL-12 gene therapy to obtain more effective therapeutic effects (Fig. 3b). Gene delivery using Bubble liposomes, ultrasound or Lipofectamine 2000 showed no apparent anti-tumor effect, even in repetitive therapy. In contrast, IL-12 gene delivery using the combination of Bubble liposomes and ultrasound effectively suppressed tumors, and complete regression occurred in 80% of the tumor-bearing mice. There was no decrease in body weight of these mice as a side effect of IL-12 cancer therapy (data not shown). In addition, this group of mice demonstrated prolonged survival, indicating that OV-HM cells were effectively killed by IL-12 gene therapy with Bubble liposomes and ultrasound.

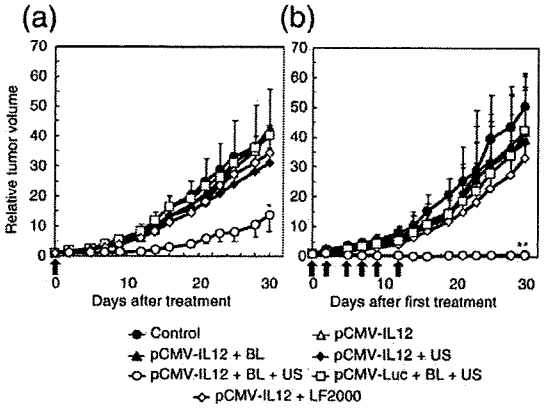

Fig. 3. Anti-tumor effect of IL-12 gene delivery. B6C3F1 mice were intradermally inoculated with 1×10^6 OV-HM cells into the flank. (a) Single gene therapy. (b) Repetitive gene therapy. Each day (arrows) after first treatment, the tumors were injected with pCMV-IL12 (10 μg) using Bubble liposomes (2.5 μg) and/or ultrasound (1 MHz, 0.7 W/cm^2, 1 min), or Lipofectamine 2000 as a conventional lipofection method. The volume of the growing tumors was calculated by: (tumor volume; mm^3) = (major axis; mm) × (minor axis; mm)^2 × 0.5). The data are represented as tumor volume relative to the tumor volume on the first day of treatment (day 7 after tumor inoculation). Arrow shows days of treatment. Each point represents the mean ± SD ($n = 5$). *$P < 0.05$ or **$P < 0.01$ compared to the group treated with pCMV-IL12, pCMV-IL12 + BL, US or LF2000 or pCMV-Luc + BL + US. BL: Bubble liposomes, US: Ultrasound, LF2000: Lipofectamine 2000.

3.4. Determination of immune subsets responsible for tumor regression induced by IL-12 gene delivery using Bubble liposomes and ultrasound

To investigate the anti-tumor mechanism of intratumoral pCMV-IL12 delivery using Bubble liposomes and ultrasound, we examined the individual contribution of CD4$^+$ and CD8$^+$ T cells and NK cells (Fig. 4). The anti-tumor effects of pCMV-IL12 delivery using Bubble liposomes and ultrasound were attenuated by the depletion of CD8$^+$ T cells and CD4$^+$ T cells. The depletion of CD8$^+$ T cells effectively blocked the anti-tumor effect. Also, the anti-tumor effect was blocked in mice that were depleted of both CD4$^+$ and CD8$^+$ T cells. On the other hand, the tumor growth suppressing effects were not affected by NK cell depletion. Therefore, we concluded that CD8$^+$ CTLs, activated by the helper function of CD4$^+$ T cells, were the predominant effector cells in this therapeutic system. CD4$^+$ cells alone also partly contributed to the enhanced anti-tumor effect.

To investigate the infiltration of CD8$^+$ T cells into tumor tissues containing the IL-12 gene delivered using Bubble liposomes and ultrasound, tumor tissues were subjected to immunohistochemical staining for CD8 (Fig. 5a–c). Tumor tissue from untreated mice, or mice treated with the IL-12 gene delivered using Bubble liposomes and ultrasound, showed increased accumulation of CD8$^+$ T cells compared to control mice treated with the luciferase gene, delivered using Bubble liposomes and ultrasound. In addition, we examined the activation states of tumor-infiltrating T cells by immunohistochemical analysis for perforin, the major cytotoxic molecule in activated CTLs (Fig. 5d–f). Tumor tissue to which the IL-12 gene had been delivered using Bubble liposomes and ultrasound exhibited significantly higher numbers of perforin-positive cells than non-treated tumor tissue, or tissue treated with luciferase gene.

4. Discussion

There are two main therapeutic strategies in cancer gene therapy. One approach is to cause a direct effect on cancer cells by delivering suicide genes such as herpes simplex virus thymidine kinase, [27] siRNA for oncogenes, [28] and proteins associated with the cell cycle [29] and apoptosis [30,31]. In this approach, it is necessary to deliver the therapeutic gene into most of the cancer cells to induce cytotoxicity. The second approach is indirect and activates anti-tumor immunity mediated by the delivery of a cytokine gene such as IL-12. In such cytokine gene therapy, the therapeutic gene does not have to be delivered into all the cancer cells since the cytokine is secreted from the cells. Therefore, a local supply of IL-12 in tumors is

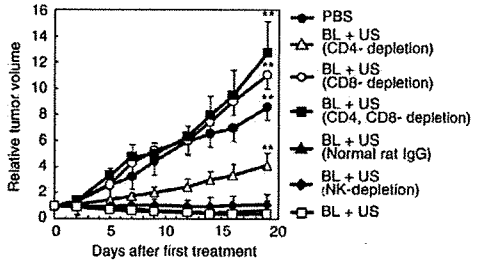

Fig. 4. Determination of immune subsets responsible for the anti-tumor effect induced by IL-12 gene delivery with Bubble liposomes and ultrasound. B6C3F1 mice were intradermally inoculated with 1×10^6 OV-HM cells into the flank. For depletion of CD4$^+$ T cells, CD8$^+$ T cells or NK cells in the mice, GK1.5 ascites (anti-CD4), 53-6.72 ascites (anti-CD8) or anti-asialoGM1 antisera was intraperitoneally injected as described in Materials and methods. On 0, 2, 5, 7, 9 or 12 days after first treatment, IL-12 gene therapy was performed with Bubble liposomes and ultrasound. The data represent the tumor volume relative to the tumor volume on the first day of treatment (day 7 after tumor inoculation). Each point represents the mean ± SD ($n = 5$). **$P < 0.01$ compared to the group treated with BL + US (Non-depletion). BL: Bubble liposomes, US: Ultrasound.

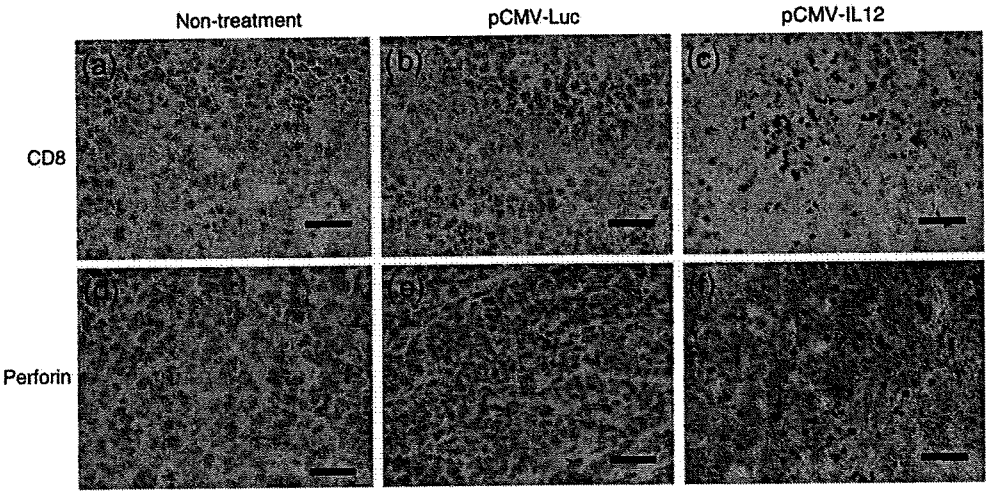

Fig. 5. Images of infiltrating T cells in OV-HM tumors following pCMV-IL12 delivery using Bubble liposomes and ultrasound. B6C3F1 mice were intradermally inoculated with 1×10^6 OV-HM cells into the flank. Seven, 9 or12 days after tumor inoculation, the tumors were injected with pCMV-Luc (b and e) or pCMV-IL12 (c and f) using Bubble liposomes and ultrasound. On day 13 after tumor inoculation, immunohistochemical staining against CD8 (a, b and c) and perforin (d, e and f) was performed using frozen tumor sections. Scale bar shows 10 μm.

an effective immunotherapeutic approach with reduced systemic adverse effects. Many anti-tumor effects depend on this method for IL-12 gene delivery. Viral vector systems have high potency and are effective for gene delivery, but gene therapy using viral vector systems may have associated safety issues [32]. Although transfection efficiency of most non-viral vector systems is lower, they are generally considered safer than viral vector systems [33]. Therefore, non-viral vector systems are preferred to cancer gene therapy using cytokines because it is not necessary to deliver the cytokine gene into all the cells. There have been many recent reports about gene delivery using the combination of nano/microbubbles and ultrasound [16–18], but most of them only confirmed the efficiency of gene expression using reporter genes. On the other hand, there have been few reports regarding therapeutic effects using sonoporation technology in cancer gene therapy. In this study, we assessed the effectiveness of the combination of Bubble liposomes and ultrasound as a non-viral vector system for effective cancer gene therapy, using plasmid DNA expressing IL-12, a potent primer of anti-tumor immunity.

IL-12 expression by IL-12 corded plasmid DNA delivery with the combination of Bubble liposomes and ultrasound was higher than that with a conventional lipofection method using Lipofectamine 2000 (Fig. 2). The therapeutic effect of IL-12 cancer gene therapy using each gene delivery method was compared (Fig. 3). IL-12 gene delivery with Lipofectamine 2000 did not suppress tumor growth, whereas gene delivery using a combination of Bubble liposomes and ultrasound effectively suppressed tumor growth. We originally thought that this was due to the level of IL-12 expression (Fig. 2), but complete tumor rejection was not observed in any mice treated with IL-12 gene delivery using Bubble liposomes and ultrasound (Fig. 3a), perhaps because the IL-12 gene is only transiently expressed in the tumor tissue. To address this problem, the IL-12 gene was repeatedly delivered using Bubble liposomes and ultrasound: as shown in Fig. 3b, the tumors were completely rejected. This complete rejection was attributed to the maintenance of therapeutic IL-12 levels in the tumor tissue. On the other hand, we could not observe anti-tumor effect in the luciferase corded plasmid DNA (pCMV-Luc) delivery with Bubble liposomes and ultrasound. This result not only suggests that IL-12 expression was important to suppress tumor growth but also suggests that there was no effect on tumor suppression by the combination of Bubble liposomes and ultrasound. In addition, we used Lipofectamine 2000 as control because gene transfection with intraperitoneal injection of Lipofectamine 2000 could effectively deliver into ascites tumor cells in our previous report [20]. Therefore, in this case of local tumoral injection, we thought that Lipofectamine 2000 could also be utilized as control vector system. Moreover, our collaborator reported about anti-tumor effects by single intratumoral injection of IL-12 expressing RGD fiber mutant adenovirus vector in OV-HM tumor bearing mice. In the report, tumor growth was suppressed and the tumor regression rate was about 40% [9]. In our study, although effective tumor growth suppression was observed in the therapeutic mice by single injection of IL-12 gene with Bubble liposomes and ultrasound, the tumor regressing mice were not observed. In this single therapy, our system was not equal to adenovirus vector in terms of tumor regression rate. On the other hand, the tumor regression rate in our repetitive therapy reached to 80%. And anti-tumor effect by repetitive therapy in our gene delivery system could go beyond that by single therapy with adenovirus vector. From these results, it was thought that the combination of Bubble liposomes and ultrasound might be a useful non-viral vector system for cancer gene therapy.

The anti-tumor effect by gene delivery with the combination of Bubble liposomes and ultrasound completely disappeared in mice lacking $CD8^+$ T lymphocytes (Fig. 4). Therefore, in this IL-12 gene therapy, $CD8^+$ T lymphocytes play a major role in suppressing tumor growth, suggesting that the combination of Bubble liposomes and ultrasound can effectively induce sufficient IL-12 expression to cause anti-tumor immune responses. In the Fig. 4, $CD8^+$ T lymphocytes depletion and $CD4^+$ and $CD8^+$ T lymphocytes depletion rather enhanced tumor growth. We thought that this reason was a same phenomenon as increasing the frequency of tumor generation according to decrease anti-tumor activity of immune competent cells by immunosuppressive agents. In brief, the balance of tumor growth and tumor rejection by immune system trend toward tumor growth by the depletion of $CD4^+$ and $CD8^+$ T lymphocytes. Therefore, it was thought that tumor growth was accelerated by the depletion. In other report, same phenomenon was observed [34]. The invasion of many $CD8^+$ T lymphocytes was observed in tumor tissue from mice treated with the IL-12 gene, Bubble liposomes and ultrasound (Fig. 5c), and perforin-positive cells were also observed in this tumor tissue (Fig. 5f). These results suggest that the expression of IL-12 genes, delivered using Bubble liposomes and ultrasound, primed the anti-tumor immunity, causing the tumor cells to be rejected. In this study, we did not measure the IL-12 concentration in the tumor tissue, but Colombo et al. reported that 30–80 pg/ml IL-12 at the tumor site can induce 40% regression of

C26 colon carcinoma [8]. Although the therapeutic effect depends on the type of cancer, we estimate that IL-12 concentrations of the order of tens of pg/ml are expressed at the tumor site using the present therapeutic system.

In conclusion, we demonstrated that the combination of Bubble liposomes and ultrasound effectively delivers the IL-12 gene into tumor tissue, and that local IL-12 production induces an immune response to the tumor cells. Therefore, the combination of Bubble liposomes and ultrasound could be a useful non-viral vector system in cancer gene therapy.

Acknowledgements

We thank Dr. Hiroshi Yamamoto (Department of Immunology, Graduate School of Pharmaceutical Sciences, Osaka University, Japan) for providing mIL-12 BIA/pBluescript II KS(−). We are grateful to Dr. Katsuro Tachibana (Department of Anatomy, School of Medicine, Fukuoka University, Japan) and Dr. Nobuki Kudo (Laboratory of Biomedical Instrumentation and Measurements, Graduate School of Information Science and Technology, Hokkaido University, Japan) for technical advice regarding the induction of cavitation with ultrasound exposure, to Dr. Yasuhiro Matsumura (Investigative Treatment Division, Research Center for Innovative Oncology, National Cancer Center Hospital East, Japan) for technical advice about cancer therapy, to Mr. Yasuyuki Shiono, Mr. Ryo Tanakadate, Mr. Kunihiko Matsuo, Mr. Ken Osawa and Ms. Motoka Kawamura (Department of Biopharmaceutics, School of Pharmaceutical Sciences, Teikyo University, Japan) for technical assistance, and to Mr. Yasuhiko Hayakawa, Mr. Takahiro Yamauchi and Mr. Kosho Suzuki (Nepa Gene Co., Ltd., Chiba, Japan) for technical advice about ultrasound exposure.

This study was supported by Grant-in-Aid for Young Scientists (B) from the Ministry of Education, Culture, Sports, Science and Technology of Japan, Grant-in-Aid for Scientific Research (A) and (B) from the Japan Society for the Promotion of Science, and Health and Labour Sciences Research Grants, Third Term Comprehensive Control Research for Cancer from the Ministry of Health, Labour and Welfare.

References

[1] U. Gubler, A.O. Chua, D.S. Schoenhaut, C.M. Dwyer, W. McComas, R. Motyka, N. Nabavi, A.G. Wolitzky, P.M. Quinn, P.C. Familletti, Coexpression of two distinct genes is required to generate secreted bioactive cytotoxic lymphocyte maturation factor, Proc Natl Acad Sci U S A 88 (1991) 4143–4147.
[2] S.F. Wolf, P.A. Temple, M. Kobayashi, D. Young, M. Dicig, L. Lowe, R. Dzialo, L. Fitz, C. Ferenz, R.M. Hewick, Cloning of cDNA for natural killer cell stimulatory factor, a heterodimeric cytokine with multiple biologic effects on T and natural killer cells, J Immunol 146 (1991) 3074–3081.
[3] M.J. Brunda, Interleukin-12, J Leukoc Biol 55 (1994) 280–288.
[4] C.L. Nastala, H.D. Edington, T.G. McKinney, H. Tahara, M.A. Nalesnik, M.J. Brunda, M.K. Gately, S.F. Wolf, R.D. Schreiber, W.J. Storkus, Recombinant IL-12 administration induces tumor regression in association with IFN-gamma production, J Immunol 153 (1994) 1697–1706.
[5] W.G. Yu, M. Ogawa, J. Mu, K. Umehara, T. Tsujimura, H. Fujiwara, T. Hamaoka, IL-12-induced tumor regression correlates with in situ activity of IFN-gamma produced by tumor-infiltrating cells and its secondary induction of anti-tumor pathways, J Leukoc Biol 62 (1997) 450–457.
[6] M.B. Atkins, M.J. Robertson, M. Gordon, M.T. Lotze, M. DeCoste, J.S. DuBois, J. Ritz, A.B. Sandler, H.D. Edington, P.D. Garzone, J.W. Mier, C.M. Canning, L. Battiato, H. Tahara, M.L. Sherman, Phase I evaluation of intravenous recombinant human interleukin 12 in patients with advanced malignancies, Clin Cancer Res 3 (1997) 409–417.
[7] J.P. Leonard, M.L. Sherman, G.L. Fisher, L.J. Buchanan, G. Larsen, M.B. Atkins, J.A. Sosman, J.P. Dutcher, N.J. Vogelzang, J.L. Ryan, Effects of single-dose interleukin-12 exposure on interleukin-12-associated toxicity and interferon-gamma production, Blood 90 (1997) 2541–2548.
[8] M.P. Colombo, M. Vagliani, F. Spreafico, M. Parenza, C. Chiodoni, C. Melani, A. Stoppacciaro, Amount of interleukin 12 available at the tumor site is critical for tumor regression, Cancer Res 56 (1996) 2531–2534.
[9] J.Q. Gao, T. Sugita, N. Kanagawa, K. Iida, Y. Eto, Y. Motomura, H. Mizuguchi, Y. Tsutsumi, T. Hayakawa, T. Mayumi, S. Nakagawa, A single intratumoral injection of a fiber-mutant adenoviral vector encoding interleukin 12 induces remarkable anti-tumor and anti-metastatic activity in mice with Meth-A fibrosarcoma, Biochem Biophys Res Commun 328 (2005) 1043–1050.
[10] Y. Gao, Z. Xu, S. Chen, W. Gu, L. Chen, Y. Li, Arginine-chitosan/DNA self-assemble nanoparticles for gene delivery: in vitro characteristics and transfection efficiency, Int J Pharm 359 (2008) 241–246.
[11] H. Hatakeyama, H. Akita, K. Kogure, M. Oishi, Y. Nagasaki, Y. Kihira, M. Ueno, H. Kobayashi, H. Kikuchi, H. Harashima, Development of a novel systemic gene delivery system for cancer therapy with a tumor-specific cleavable PEG-lipid, Gene Ther 14 (2007) 68–77.
[12] T. Montier, T. Benvegnu, P.A. Jaffres, J.J. Yaouanc, P. Lehn, Progress in cationic lipid-mediated gene transfection: a series of bio-inspired lipids as an example, Curr Gene Ther 8 (2008) 296–312.
[13] M. Morille, C. Passirani, A. Vonarbourg, A. Clavreul, J.P. Benoit, Progress in developing cationic vectors for non-viral systemic gene therapy against cancer, Biomaterials 29 (2008) 3477–3496.
[14] M. Fechheimer, J.F. Boylan, S. Parker, J.E. Sisken, G.L. Patel, S.G. Zimmer, Transfection of mammalian cells with plasmid DNA by scrape loading and sonication loading, Proc Natl Acad Sci U S A 84 (1987) 8463–8467.
[15] M.W. Miller, D.L. Miller, A.A. Brayman, A review of in vitro bioeffects of inertial ultrasonic cavitation from a mechanistic perspective, Ultrasound Med Biol 22 (1996) 1131–1154.
[16] C.M. Newman, T. Bettinger, Gene therapy progress and prospects: ultrasound for gene transfer, Gene Ther 14 (2007) 465–475.
[17] Z.P. Shen, A.A. Brayman, L. Chen, C.H. Miao, Ultrasound with microbubbles enhances gene expression of plasmid DNA in the liver via intraportal delivery, Gene Ther 15 (2008) 1147–1155.
[18] Y. Taniyama, K. Tachibana, K. Hiraoka, T. Namba, K. Yamasaki, N. Hashiya, M. Aoki, T. Ogihara, K. Yasufumi, R. Morishita, Local delivery of plasmid DNA into rat carotid artery using ultrasound, Circulation 105 (2002) 1233–1239.
[19] R. Suzuki, T. Takizawa, Y. Negishi, K. Hagisawa, K. Tanaka, K. Sawamura, N. Utoguchi, T. Nishioka, K. Maruyama, Gene delivery by combination of novel liposomal bubbles with perfluoropropane and ultrasound, J Control Release 117 (2007) 130–136.
[20] R. Suzuki, T. Takizawa, Y. Negishi, N. Utoguchi, K. Sawamura, K. Tanaka, E. Namai, Y. Oda, Y. Matsumura, K. Maruyama, Tumor specific ultrasound enhanced gene transfer in vivo with novel liposomal bubbles, J Control Release 125 (2008) 137–144.
[21] R. Suzuki, Y. Oda, N. Utoguchi, E. Namai, Y. Taira, N. Okada, N. Kadowaki, T. Kodama, K. Tachibana, K. Maruyama, A novel strategy utilizing ultrasound for antigen delivery in dendritic cell-based cancer immunotherapy, J Control Release 133 (2009) 198–205.
[22] T. Yamashita, S. Sonoda, R. Suzuki, N. Arimura, K. Tachibana, K. Maruyama, T. Sakamoto, A novel bubble liposome and ultrasound-mediated gene transfer to ocular surface: RC-1 cells in vitro and conjunctiva in vivo, Exp Eye Res 85 (2007) 741–748.
[23] Y. Negishi, Y. Endo, T. Fukuyama, R. Suzuki, T. Takizawa, D. Omata, K. Maruyama, Y. Aramaki, Delivery of siRNA into the cytoplasm by liposomal bubbles and ultrasound, J Control Release 132 (2008) 124–130.
[24] K. Un, S. Kawakami, R. Suzuki, K. Maruyama, F. Yamashita, M. Hashida. Enhanced transfection efficiency into macrophages and dendritic cells by the combination method using mannosylated lipoplexes and Bubble liposomes with ultrasound exposure Hum Gene Ther. (2009) In press.
[25] M. Hashimoto, O. Niwa, Y. Nitta, M. Takeichi, K. Yokoro, Unstable expression of E-cadherin adhesion molecules in metastatic ovarian tumor cells, Jpn J Cancer Res 80 (1989) 459–463.
[26] Y. Okada, N. Okada, S. Nakagawa, H. Mizuguchi, M. Kanehira, N. Nishino, K. Takahashi, N. Mizuno, T. Hayakawa, T. Mayumi, Fiber-mutant technique can augment gene transduction efficacy and anti-tumor effects against established murine melanoma by cytokine-gene therapy using adenovirus vectors, Cancer Lett 177 (2002) 57–63.
[27] C. Fillat, M. Carrio, A. Cascante, B. Sangro, Suicide gene therapy mediated by the Herpes Simplex virus thymidine kinase gene/Ganciclovir system: fifteen years of application, Curr Gene Ther 3 (2003) 13–26.
[28] X.H. Shi, Z.Y. Liang, X.Y. Ren, T.H. Liu, Combined silencing of K-ras and Akt2 oncogenes achieves synergistic effects in inhibiting pancreatic cancer cell growth in vitro and in vivo, Cancer Gene Ther 16 (2009) 227–236.
[29] M. Nogawa, T. Yuasa, S. Kimura, M. Tanaka, J. Kuroda, K. Sato, A. Yokota, H. Segawa, Y. Toda, S. Kageyama, T. Yoshiki, Y. Okada, T. Maekawa, Intravesical administration of small interfering RNA targeting PLK-1 successfully prevents the growth of bladder cancer, J Clin Invest 115 (2005) 978–985.
[30] C.W. Beh, W.Y. Seow, Y. Wang, Y. Zhang, Z.Y. Ong, P.L. Ee, Y.Y. Yang, Efficient delivery of Bcl-2-targeted siRNA using cationic polymer nanoparticles: down-regulating mRNA expression level and sensitizing cancer cells to anticancer drug, Biomacromolecules 10 (2009) 41–48.
[31] M. Folini, M. Pennati, N. Zaffaroni, RNA interference-mediated validation of genes involved in telomere maintenance and evasion of apoptosis as cancer therapeutic targets, Methods Mol Biol 487 (2009) 303–330.
[32] S. Lehrman, Virus treatment questioned after gene therapy death, Nature 401 (1999) 517–518.
[33] C.C. Conwell, L. Huang, Recent advances in non-viral gene delivery, Adv Genet 53PA (2005) 1–18.
[34] N. Kanagawa, J.Q. Gao, Y. Motomura, T. Yanagawa, Y. Mukai, Y. Yoshioka, N. Okada, S. Nakagawa, Antitumor mechanism of intratumoral injection with IL-12-expressing adenoviral vector against IL-12-unresponsive tumor, Biochem Biophys Res Commun 372 (2008) 821–825.